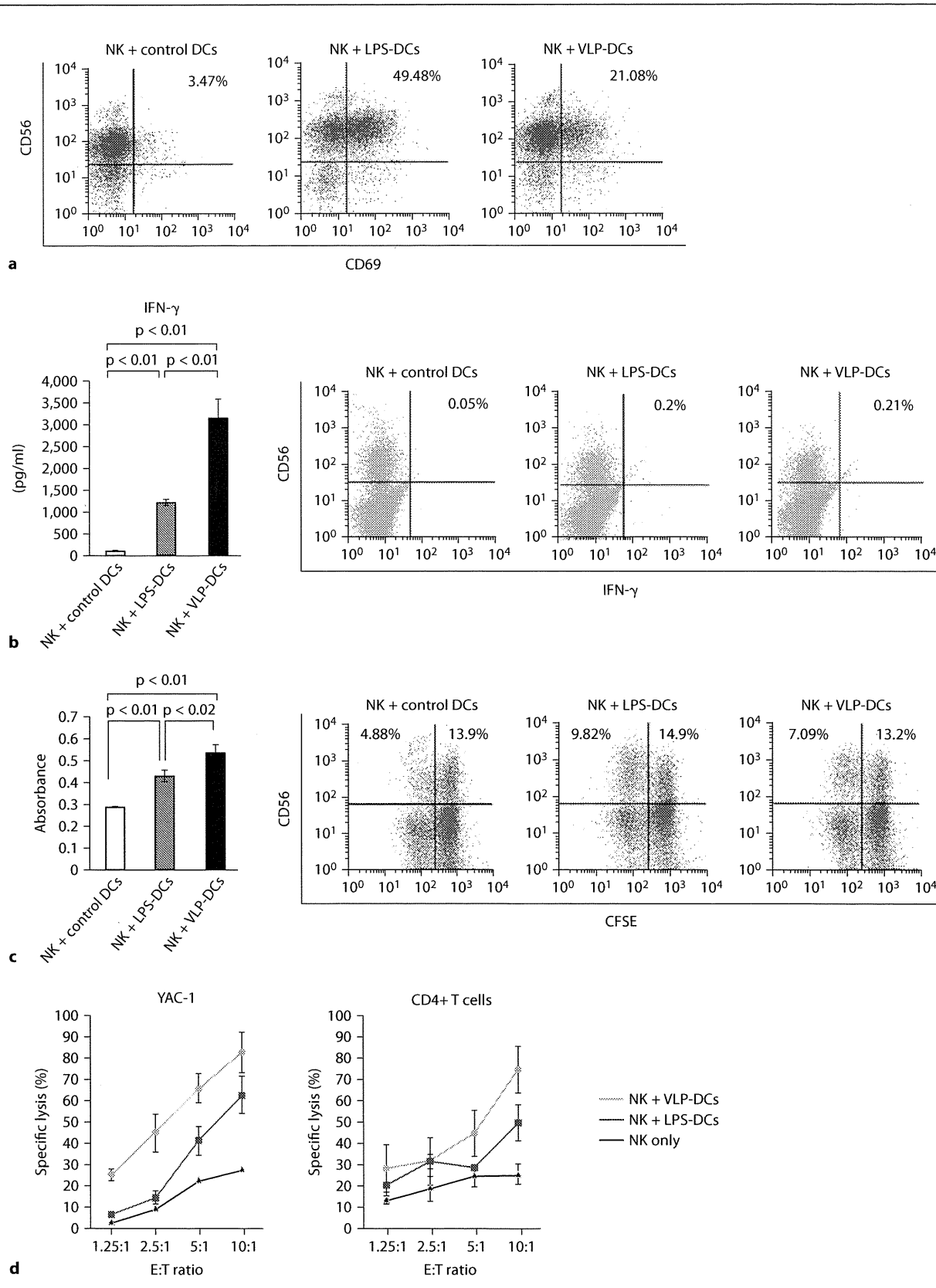

Color version available online

2

In conclusion, we show that Gag-VLPs efficiently activate human MDDCs in vitro and murine DCs in vivo. Furthermore, VLP-activated DCs subsequently induce innate immune responses as well as HIV-1-Gag-specific immune responses in NK cells.

Discussion

Despite extensive efforts to combat AIDS, the global HIV-infected population continues to increase on a daily basis. Highly active antiretroviral therapy results in significant suppression of HIV viral load but is unable to eradicate the virus from the body because of the appearance of resistant strains. One of the greatest hopes for preventing HIV infection and progression to AIDS is the development of an effective prophylactic or therapeutic vaccine.

In recent years, Gag-VLPs have been shown to be highly attractive HIV vaccine candidates because of their ability to activate multiple cell types such as DCs, T cells and B cells [9, 15, 16]. In this report, we used an HIV-1 Gag-VLP as an immunogen in a vaccine against HIV to induce DC-mediated NK cell immune responses. Previous reports showed that HIV envelope glycoprotein 120 (Env-gp120)-containing VLPs mainly induced Th2-polarizing cytokines (IL-6, IL-10 and TNF-α) and failed to induce significant levels of Th1-polarizing cytokines (IL-12 p70 and IFN-γ). The high levels of IL-10 and TNF-α induced by Env-VLPs could explain the aberrant function of immature DCs and impairment of T cell proliferation [32]. Moreover, gp120 induces production of IL-4, which drives synthesis of IgE and inhibits synthesis of antiviral IgG by B cells, inactivation of Th1 cells and inhibition of CTL responses [33]. The results from phase III trials showed that purified recombinant Env-gp120 failed to protect against HIV-1 infection and also failed to induce production of neutralizing antibodies to diverse primary isolates. The presence of HIV-1 Env-gp120 in Gag-VLPs switches the Th2 polarization in peripheral blood mononuclear cells from HIV-infected subjects [34–36]. For these reasons, HIV-1 Gag-VLPs are preferred as an HIV-1 vaccine candidate.

Internalization of VLPs into DCs occurs through actin-dependent macropinocytosis and endocytosis. VLP uptake is also induced by DC-SIGN-mediated endocytosis. The ability of Gag-VLPs to target DCs is an important advantage over other HIV vaccines because activation of DCs is essential for the induction of subsequent innate and adaptive immune responses. Although numerous reports have demonstrated Gag-VLP-mediated induction of $CD4^+$ T cell activation, CTL responses and B-cell-mediated humoral immunity, reports on the induction of NK cell immune responses by Gag-VLPs are virtually absent.

Recent reports indicate that long-term non-progressing HIV-1 infection does not necessarily require the presence of broadly cross-reactive neutralizing antibodies; however, a strong antiviral cytotoxic activity has been shown to correlate temporally with the clearance of viremia during primary infection [37]. In contrast, reports showing a negative correlation between the number of Gag-specific $CD8^+$ T cells and HIV viral load or progression to AIDS made it necessary to reevaluate the efficiency of HIV vaccines [38]. Recently, it became apparent that a $CD8^+$ T cell-inducing vaccine failed in a phase IIB clinical trial. The trial was suspended after an interim analysis showed that the vaccine did not protect the trial participants against HIV infection and indicated that the presence of high numbers of cytokine-producing HIV-specific $CD8^+$ T cells does not guarantee a better clinical outcome [39]. Taken together,

Fig. 3. Immunization of mice with Gag-VLPs and assessment of DC and NK cell activation. **a** Schematic representation of the phase I and phase II immunization regimens. In phase I immunizations, 4 groups of female BALB/c mice, each consisting of 3 subgroups with 4 animals, were immunized by intramuscular (i.m.) injection of 50 μg of Gag-VLPs or 1 μg of LPS or were left untreated. Twenty-four hours after priming, mice from the first group were sacrificed and their spleens were collected for analysis of DC and NK cell activation. The remaining groups of mice were given first booster injections using the same doses 7 days after priming. Mice from the second group were sacrificed after 24 h and their spleens were collected. Mice from the third and fourth groups were given a second booster injection on day 14. After 24 h, mice from the third group (donor mice) were sacrificed, and blood samples were collected for the quantification of serum IFN-γ by ELISA. Spleens were removed for flow cytometry analysis. At the same time, splenic DCs were purified using a mouse $CD11c^+$ DC isolation kit (Miltenyi Biotec) and subsequently used in phase II immunizations. Mice from the fourth group were sacrificed 3 weeks after the second booster injection, and spleens were collected for flow cytometry. A portion of splenocytes was restimulated overnight with 5 μg/ml Gag-VLPs and used for intracellular staining of IFN-γ-producing NK cells and ex vivo cytotoxicity assays. In phase II immunizations, 4 groups of (recipient) BALB/c mice, each consisting of 5 animals, were adoptively transferred with purified splenic DCs (1×10^6 cells/mouse) from phase I-immunized (donor) mice from the third group. After 24 h, all mice were sacrificed and sera and spleens were collected for immunological assays. **b** Expression of mouse CD80, CD86 and MHC I and MHC II molecules on splenic DCs from the first group of phase I-immunized mice was analyzed by flow cytometry.

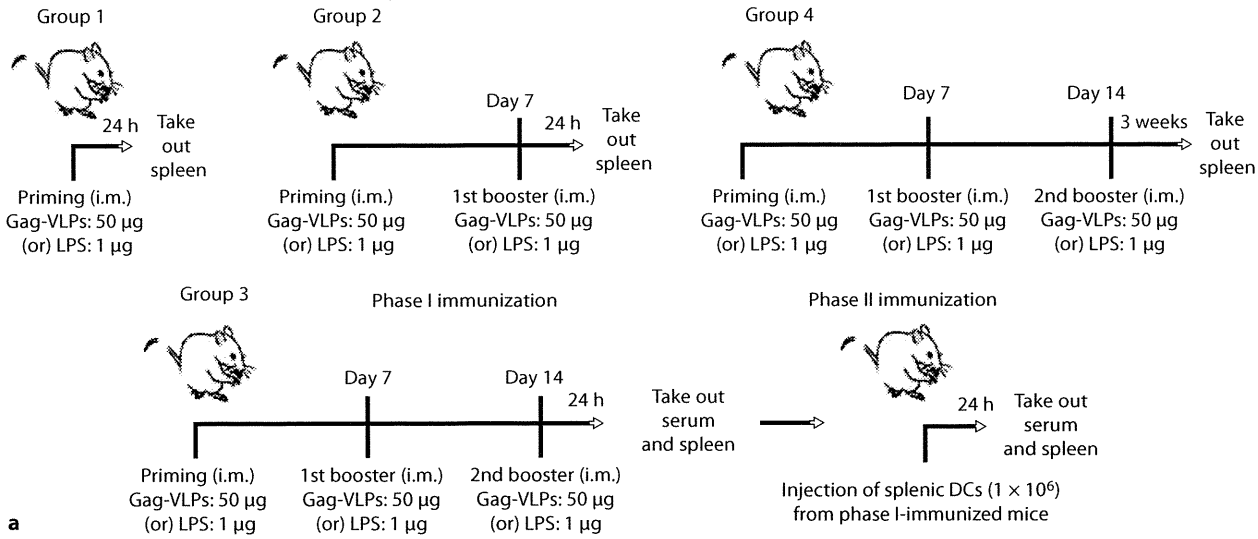
Group 1
24 h
Take out spleen
Priming (i.m.)
Gag-VLPs: 50 μg
(or) LPS: 1 μg
Group 2
Day 7
24 h
Take out spleen
Priming (i.m.)
Gag-VLPs: 50 μg
(or) LPS: 1 μg
1st booster (i.m.)
Gag-VLPs: 50 μg
(or) LPS: 1 μg
Group 4
Day 7
Day 14
3 weeks
Take out spleen
Priming (i.m.)
Gag-VLPs: 50 μg
(or) LPS: 1 μg
1st booster (i.m.)
Gag-VLPs: 50 μg
(or) LPS: 1 μg
2nd booster (i.m.)
Gag-VLPs: 50 μg
(or) LPS: 1 μg
Group 3
Phase I immunization
Day 7
Day 14
24 h
Take out serum and spleen
Priming (i.m.)
Gag-VLPs: 50 μg
(or) LPS: 1 μg
1st booster (i.m.)
Gag-VLPs: 50 μg
(or) LPS: 1 μg
2nd booster (i.m.)
Gag-VLPs: 50 μg
(or) LPS: 1 μg
Phase II immunization
24 h
Take out serum and spleen
Injection of splenic DCs (1 × 10⁶) from phase I-immunized mice

a

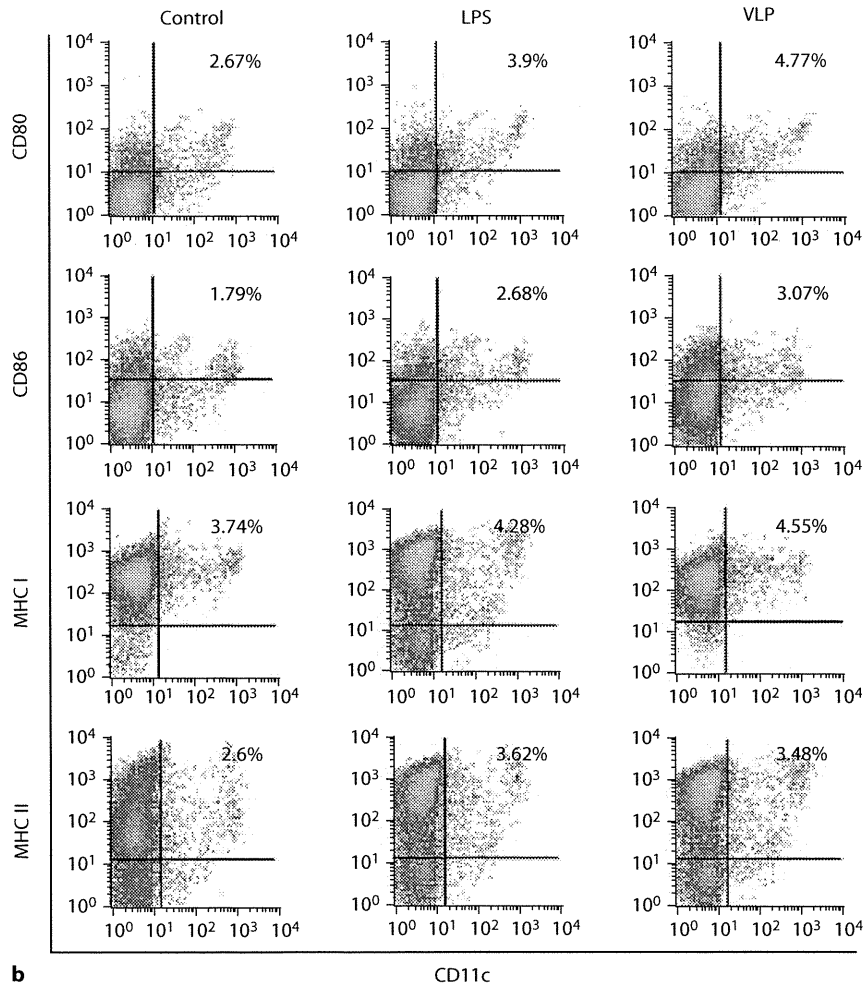
Control
LPS
VLP
CD80
CD86
MHC I
MHC II
2.67%
3.9%
4.77%
1.79%
2.68%
3.07%
3.74%
4.28%
4.55%
2.6%
3.62%
3.48%
CD11c

b

3

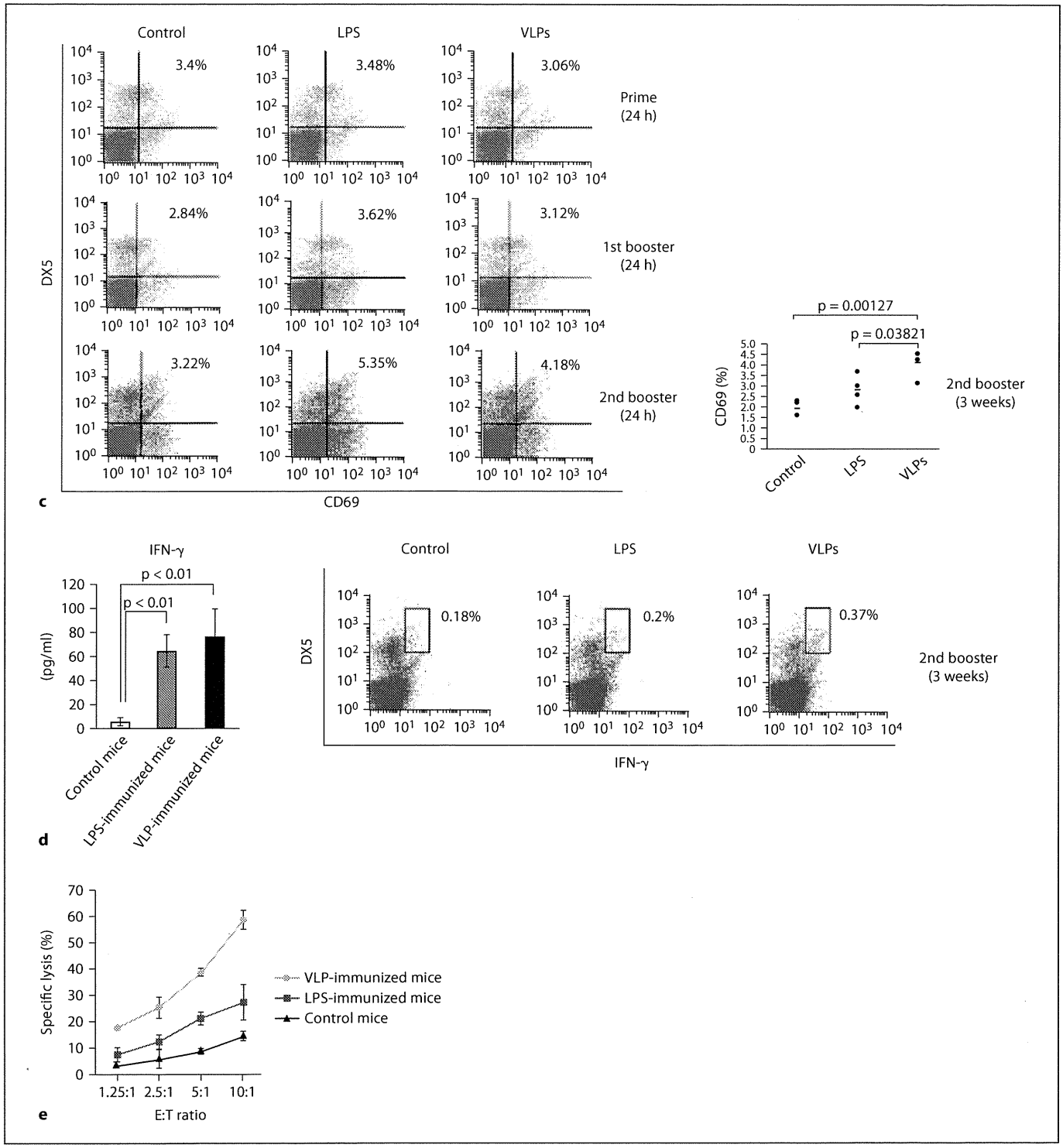

Color version available online

Fig. 3. Immunization of mice with Gag-VLPs and assessment of DC and NK cell activation. **c** CD69 expression on NK cells from each group of phase I-immunized mice was analyzed by flow cytometry. **d** Serum IFN-γ levels from the third group of phase I-immunized mice were determined by ELISA. IFN-γ-producing splenic NK cells from the fourth group of phase I-immunized mice after restimulation with Gag-VLPs were examined by intracellular cytokine staining. The results are representative of 3 independent experiments. **e** Gag-specific NK cell cytolysis of Gag-VLP-loaded spleen cells was assessed by measuring LDH release using the Cytotox 96 non-radioactive cytotoxicity assay kit. The results are expressed as means ± SD of triplicate cultures. Comparable results were obtained in 2 independent experiments. E:T = Effector to target.

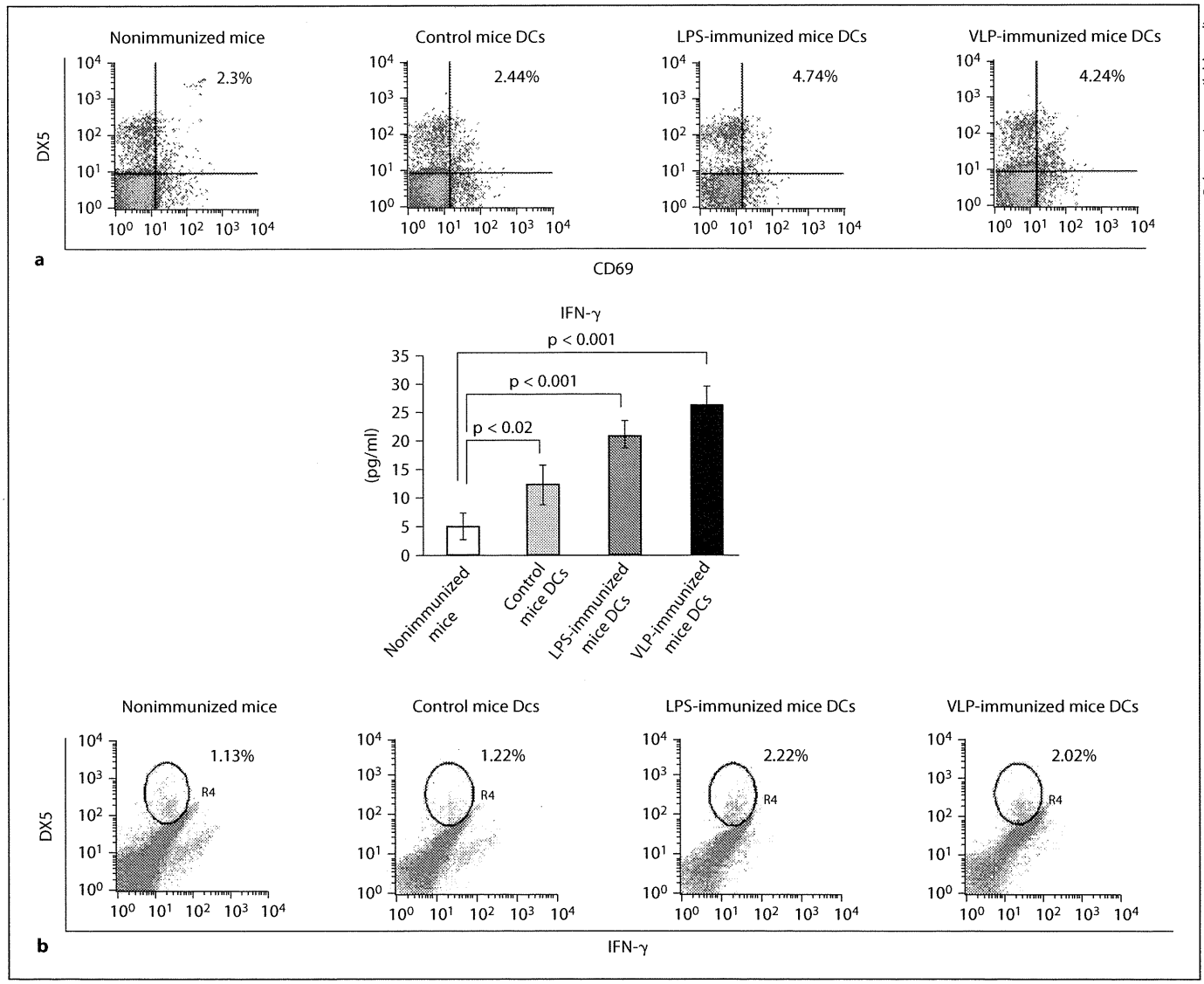

Fig. 4. DCs from phase I-immunized donor mice induce in vivo activation of NK cells. **a** NK cell activation in phase II, DC-immunized recipient mice was analyzed by flow cytometry after staining the spleen cells with antibodies against DX5-PE and anti-CD69-FITC. **b** Serum IFN-γ levels of phase II-immunized or control mice were determined using a mouse IFN-γ ELISA assay kit. All results are expressed as means ± SD of triplicate wells. Statistical analysis was performed using Student's t test. IFN-γ-producing murine NK cells were examined by intracellular cytokine staining and FACS analysis. The results are representative of 3 independent experiments.

these results suggest that in order to achieve an effective potential HIV vaccine, a strategy that results in induction of both nonspecific innate immune responses and specific immune responses against HIV is necessary.

In this study, we first demonstrated the activation of DCs and NK cells by Gag-VLPs both in vitro and in vivo by immunization with Gag-VLPs or splenic DCs isolated from VLP-immunized mice in a 2-phase immunization experiment.

We generated HIV-1 Gag-VLPs in mammalian HeLa cells to exclude the possible baculovirus contamination of VLP preparations, which may have affected the results of experiments intended to analyze the immunogenicity of VLPs. Our studies using these VLP preparations showed that incubation of human MDDCs with Gag-VLPs resulted in upregulation of the DC maturation markers MHC I and MHC II and of costimulatory molecules such as CD80 and CD86 (fig. 1a). DC activation is

also characterized by the production of cytokines that are important for the priming of innate and adaptive immune cells such as NK cells, $CD4^+$ and $CD8^+$ T cells. Thus, to determine the type of responses elicited by DCs stimulated with VLPs, we examined the secretion of IL-12 p70, IL-15, TNF-α, IFN-α and IFN-γ in culture supernatants and demonstrated that Gag-VLP-treated DCs produced increased levels of cytokines (fig. 1b). The quality and the quantity of DCs are important factors when attempting to induce effective immune responses in T cells and NK cells. To be effective, a vaccine must restore both the function and the number of DCs in HIV-infected persons. In vivo expansion of DCs after immunization has been shown to be necessary for the activation of other immune cells [16]. Moreover, since DC immunotherapy requires a sufficient quantity of functional autologous DCs, it is important that stimulation with Gag-VLPs should induce the activation and maturation of DCs as well as proliferation of functional DCs. We next used 2 methods to investigate the ability of Gag-VLPs to induce proliferation of human DCs in vitro. The results of CFSE labeling experiments and experiments using a proliferation assay kit both demonstrated the proliferation of VLP-treated MDDCs (fig. 1c). To further prove the capability of VLP-treated DCs to stimulate NK cells, coculture experiments were performed to analyze NK cell immune responses. These experiments demonstrated that NK cells cocultured with VLP-treated DCs showed upregulation of CD69 expression, IFN-γ production, proliferation and cytotoxicity against YAC-1 cells and HIV-infected CD4+ T cells (fig. 2). Furthermore, MDDCs produced IFN-γ after stimulation with Gag-VLPs or LPS, but the presence of NK cells in cocultures significantly increased IFN-γ levels (about 8-fold). Because the number of DCs in cocultures was 10 times less than that in DC-only cultures, we hypothesized that the IFN-γ in NK/DC cocultures was produced mainly by NK cells.

Recent reports have demonstrated NK cell memory for specific antigens and NK cell involvement in both innate and adaptive immunity. Rapid NK cell responses during innate immune activation are also associated with long-lasting antigen-specific NK cell memory responses [40–44]. NK cells can develop memory-like properties based on prior activation. These amplified NK cell responses are important for the early response to pathogens, and it may be possible to boost the NK cell response to subsequent infection by stimuli that result in the memory-like NK cell phenotype. NK cells can orchestrate specific immune responses to infection by recognizing pathogens through germ-line-encoded receptors such as toll-like receptors [45].

In our studies, immunization of mice with Gag-VLPs resulted in activation of murine DCs and NK cells in vivo, supporting the results of in vitro experiments (fig. 3b–e). We evaluated NK cell activation 24 h after each immunization with Gag-VLPs (prime, first and second booster injections) to verify the immediate NK cell response to each immunization and again 3 weeks after the last immunization to verify Gag-specific NK cell memory as shown in figure 3d (right panel) and e. We found that the prime/boost regimen using Gag-VLPs significantly enhanced NK cell activation and Gag-specific NK cell immunity. In both LPS-immunized mice and Gag-VLP-immunized mice, nonspecific activation of NK cells was evidenced by the increase in CD69 expression shortly after (24 h) each immunization (fig. 3c). In contrast, long-lasting Gag-specific NK cell immune responses of NK cells were only seen in Gag-VLP-immunized mice (fig. 3d, right panel, e). These results demonstrate that Gag-VLPs are able to induce NK cell innate immune responses as well as HIV-1 Gag-specific memory responses.

Sailaja et al. [16] injected mice intraperitoneally with Gag-VLPs once and assessed the activation of splenic DCs, T cells and B cells on day 3. Our data showed that 24 h after priming, NK cell activation was not detected in the first group of mice. This is likely due to the early time point at which the mice were examined, a short time (24 h) after injection with Gag-VLPs, which is likely too short a time period to induce DC-mediated NK cell activation in vivo. NK cell activation was found to increase after each booster injection due to the increased activation of DCs induced by booster injections (fig. 3c).

Adoptive transfer of DCs from VLP-immunized mice in the phase II immunization experiments revealed that Gag-VLP-immunized DCs could induce NK cell innate and Gag-specific immune responses in vivo (fig. 4a, b).

In most previous adoptive transfer studies, mice were injected intraperitoneally with 1×10^6 DCs [46]. Transferred DCs reportedly localized in the spleen as early as 3 h after intravenous injection and persisted for 24 h. DCs entering the popliteal lymph nodes from the footpad were also located 3 h after subcutaneous transfer [47]. Eggert et al. [48] injected mice subcutaneously, intraperitoneally and intravenously with 1×10^6 DCs/mouse. In intravenously injected mice, DCs localized in the lung 5 min after injection and in the spleen as early as 2 h after injection. DCs were detected in the draining lymph nodes 8 h

after intraperitoneal injection [48]. DCs adhere to endothelium within the splenic marginal zone through endothelium-specific homing receptors and chemokine receptor expression [49]. The required number of DCs, DC trafficking/migration patterns and subsequent immune responses differ greatly according to cell type, route of inoculation and the immune competency of recipient mice.

In this study, we evaluated the ability of Gag-VLPs to induce NK cell innate responses and HIV-1 Gag-specific NK cell adaptive immunity, which is essential for the immunological control of HIV-1 infection. These studies highlighted the role of DCs in VLP-based vaccine strategies. Our findings have significant implications for the design of a highly effective vaccine model for prophylactic and therapeutic purposes in HIV infection.

Acknowledgements

We thank Mr. Yuuta Kasai and Miss Megumi Watanabe for helpful discussions as well as for their excellent work in performing immunizations and ELISA. This work was supported, in part, by a Grant-in-Aid for High Technology Research (No. 09309011) from the Ministry of Education, Science, Sports and Culture, Japan, by a Grant-in-Aid for AIDS research from the Ministry of Health, Labor and Welfare, Japan, by a grant from the Supporting Program for Creating University Ventures from the Science and Technology Agency, Japan, and by a grant for the Research and Development Program for New Bio-industry Initiatives from the Ministry of Agriculture, Forestry and Fisheries of Japan.

Disclosure Statement

The authors declare that they have no competing interests.

References

1 Murphey-Corb M: Live-attenuated HIV vaccines: how safe is safe enough? Nat Med 1997; 3:17–18.
2 Ruprecht RM: Live attenuated AIDS viruses as vaccines: promise or peril? Immunol Rev 1999;170:135–149.
3 Robertson JS, Griffiths E: Assuring the quality, safety, and efficacy of DNA vaccines. Mol Biotechnol 2001;17:143–149.
4 Noad R, Roy P: Virus-like particles as immunogens. Trends Microbiol 2003;11:438–444.
5 Grgacic EV, Anderson DA: Virus-like particles: passport to immune recognition. Methods 2006;40:60–65.
6 Ludwig C, Wagner R: Virus-like particles – universal molecular toolboxes. Curr Opin Biotechnol 2007;18:537–545.
7 Doan LX, Li M, Chen C, Yao Q: Virus-like particles as HIV-1 vaccines. Rev Med Virol 2005;15:75–88.
8 Young KR, McBurney SP, Karkhanis LU, Ross TM: Virus-like particles: designing an effective AIDS vaccine. Methods 2006;40: 98–117.
9 Buonaguro L, Tornesello ML, Tagliamonte M, Gallo RC, Wang LX, Kamin-Lewis R, Abdelwahab S, Lewis GK, Buonaguro FM: Baculovirus-derived human immunodeficiency virus type 1 virus-like particles activate dendritic cells and induce ex vivo T-cell responses. J Virol 2006;80:9134–9143.
10 Tsunetsugu-Yokota Y, Morikawa Y, Isogai M, Kawana-Tachikawa A, Odawara T, Nakamura T, Grassi F, Autran B, Iwamoto A: Yeast-derived human immunodeficiency virus type 1 p55(gag) virus-like particles activate dendritic cells (DCs) and induce perforin expression in Gag-specific CD8(+) T cells by cross-presentation of DCs. J Virol 2003; 77:10250–10259.
11 Morón VG, Rueda P, Sedlik C, Leclerc C: In vivo, dendritic cells can cross-present virus-like particles using an endosome-to-cytosol pathway. J Immunol 2003;171:2242–2250.
12 Deml L, Wild J, Wagner R: Virus-like particles: a novel tool for the induction and monitoring of both T-helper and cytotoxic T-lymphocyte activity. Methods Mol Med 2004;94:133–157.
13 Paliard X, Liu Y, Wagner R, Wolf H, Baenziger J, Walker CM: Priming of strong, broad, and long-lived HIV type 1 p55gag-specific $CD8^+$ cytotoxic T cells after administration of a virus-like particle vaccine in rhesus macaques. AIDS Res Hum Retroviruses 2000; 16:273–282.
14 Deml L, Speth C, Dierich MP, Wolf H, Wagner R: Recombinant HIV-1 Pr55gag virus-like particles: potent stimulators of innate and acquired immune responses. Mol Immunol 2005;42:259–277.
15 Buonaguro L, Visciano ML, Tornesello ML, Tagliamonte M, Biryahwaho B, Buonaguro FM: Induction of systemic and mucosal cross-clade neutralizing antibodies in BALB/c mice immunized with human immunodeficiency virus type 1 clade A virus-like particles administered by different routes of inoculation. J Virol 2005;79:7059–7067.
16 Sailaja G, Skountzou I, Quan FS, Compans RW, Kang SM: Human immunodeficiency virus-like particles activate multiple types of immune cells. Virology 2007;362:331–341.
17 Speth C, Bredl S, Hagleitner M, Wild J, Dierich M, Wolf H, Schroeder J, Wagner R, Deml L: Human immunodeficiency virus type-1 (HIV-1) Pr55gag virus-like particles are potent activators of human monocytes. Virology 2008;382:46–58.
18 Inaba K, Metlay JP, Crowley MT, Witmer-Pack M, Steinman RM: Dendritic cells as antigen presenting cells in vivo. Int Rev Immunol 1990;6:197–206.
19 Steinman RM, Hemmi H: Dendritic cells: translating innate to adaptive immunity. Curr Top Microbiol Immunol 2006;311:17–58.
20 Steinman RM, Banchereau J: Taking dendritic cells into medicine. Nature 2007;449: 419–426.
21 Zitvogel L: Dendritic and natural killer cells cooperate in the control/switch of innate immunity. J Exp Med 2002;195:F9–F14.
22 Cooper MA, Fehniger TA, Fuchs A, Colonna M, Caligiuri MA: NK cell and DC interactions. Trends Immunol 2004;25:47–52.
23 Moretta A: The dialogue between human natural killer cells and dendritic cells. Curr Opin Immunol 2005;17:306–311.
24 Brilot F, Strowig T, Munz C: NK cells interactions with dendritic cells shape innate and adaptive immunity. Front Biosci 2008;13: 6443–6454.
25 Wehner R, Dietze K, Bachmann M, Schmitz M: The bidirectional crosstalk between human dendritic cells and natural killer cells. J Innate Immun 2011;3:258–263.
26 Andoniou CE, Coudert JD, Degli-Esposti MA: Killers and beyond: NK-cell-mediated control of immune responses. Eur J Immunol 2008;38:2938–2942.
27 Brandstadter JD, Yang Y: Natural killer cell responses to viral infection. J Innate Immun 2011;3:274–279.
28 Guilmot A, Hermann E, Braud VM, Carlier Y, Truyens C: Natural killer cell responses to infections in early life. J Innate Immun 2011; 3:280–288.

29 Kottilil S, Chun TW, Moir S, Liu S, McLaughlin M, Hallahan CW, Maldarelli F, Corey L, Fauci AS: Innate immunity in human immunodeficiency virus infection: effect of viremia on natural killer cell function. J Infect Dis 2003;187:1038–1045.
30 Fauci AS, Mavilio D, Kottilil S: NK cells in HIV infection: paradigm for protection or targets for ambush. Nat Rev Immunol 2005; 5:835–843.
31 Osada T, Clay T, Hobeika A, Lyerly HK, Morse MA: NK cell activation by dendritic cell vaccine: a mechanism of action for clinical activity. Cancer Immunol Immunother 2006;55:1122–1131.
32 Fantuzzi L, Purificato C, Donato K, Belardelli F, Gessani S: Human immunodeficiency virus type 1 gp120 induces abnormal maturation and functional alterations of dendritic cells: a novel mechanism for AIDS pathogenesis. J Virol 2004;78:9763–9772.
33 Becker Y: HIV-1 induced AIDS is an allergy and the allergen is the Shed gp120 – a review, hypothesis, and implications. Virus Genes 2004;28:319–331.
34 Burton DR, Desrosiers RC, Doms RW, Koff WC, Kwong PD, Moore JP, Nabel GJ, Sodroski J, Wilson IA, Wyatt RT: HIV vaccine design and the neutralizing antibody problem. Nat Immunol 2004;5:233–236.
35 Buonaguro L, Tornesello ML, Gallo RC, Marincola FM, Lewis GK, Buonaguro FM: Th2 polarization in peripheral blood mononuclear cells from human immunodeficiency virus (HIV)-infected subjects, as activated by HIV virus-like particles. J Virol 2009; 83:304–313.
36 Cohen J: HIV/AIDS. Vaccine results lose significance under scrutiny. Science 2003;299: 1495.
37 Harrer T, Harrer E, Kalams SA, Elbeik T, Staprans SI, Feinberg MB, Cao Y, Ho DD, Yilma T, Caliendo AM, Johnson RP, Buchbinder SP, Walker BD: Strong cytotoxic T cell and weak neutralizing antibody response in a subset of persons with stable nonprogression HIV type I infection. AIDS Res Hum Retroviruses 1996;12:585–592.
38 Schellens IM, Borghans JA, Jansen CA, De Cuyper IM, Geskus RB, van Baarle D, Miedema F: Abundance of early functional HIV-specific $CD8^+$ T cells does not predict AIDS-free survival time. PLoS One 2008;3:e2745.
39 Vaccination and enrollment are discontinued in phase II trials of Merck's investigational HIV vaccine candidate. Press release from Merck and the HIV Vaccine Trials Network, Sept 21, 2007. http://www.hvtn.org/pdf/FINAL_HIV_Vaccine_Press_Release.pdf.
40 Cooper MA, Colonna M, Yokoyama WM: Hidden talents of natural killers: NK cells in innate and adaptive immunity. EMBO Rep 2009;10:1103–1110.
41 Cooper MA, Yokoyama WM: Memory-like responses of natural killer cells. Immunol Rev 2010;235:297–305.
42 Sun JC, Beilke JN, Lanier LL: Adaptive immune features of natural killer cells. Nature 2009;457:557–561.
43 Ugolini S, Vivier E: Immunology: natural killer cells remember. Nature 2009;457:544–545.
44 Paust S, Senman B, von Andrian UH: Adaptive immune responses mediated by natural killer cells. Immunol Rev 2010;235:286–296.
45 Janeway CA Jr, Medzhitov R: Innate immune recognition. Annu Rev Immunol 2002;20: 197–216.
46 Yoshida O, Akbar F, Miyake T, Abe M, Matsuura B, Hiasa Y, Onji M: Impaired dendritic cell functions because of depletion of natural killer cells disrupt antigen-specific immune responses in mice: restoration of adaptive immunity in natural killer-depleted mice by antigen-pulsed dendritic cell. Clin Exp Immunol 2008;152:174–181.
47 Austyn JM, Kupiec-Weglinski JW, Hankins DF, Morris PJ: Migration patterns of dendritic cells in the mouse. Homing to T cell-dependent areas of spleen, and binding within marginal zone. J Exp Med 1988;167:646–651.
48 Eggert AA, Schreurs MW, Boerman OC, Oyen WJ, de Boer AJ, Punt CJ, Figdor CG, Adema GJ: Biodistribution and vaccine efficiency of murine dendritic cells are dependent on the route of administration. Cancer Res 1999;59:3340–3345.
49 Barratt-Boyes SM, Zimmer MI, Harshyne LA, Meyer EM, Watkins SC, Capuano S 3rd, Murphey-Corb M, Falo LD Jr, Donnenberg AD: Maturation and trafficking of monocyte-derived dendritic cells in monkeys: implications for dendritic cell-based vaccines. J Immunol 2000;164:2487–2495.

THE JOURNAL OF BIOLOGICAL CHEMISTRY VOL. 286, NO. 12, pp. 10051–10057, March 25, 2011

Heat Shock Protein 70 Inhibits HIV-1 Vif-mediated Ubiquitination and Degradation of APOBEC3G*

Received for publication, July 19, 2010, and in revised form, January 10, 2011 Published, JBC Papers in Press, January 12, 2011, DOI 10.1074/jbc.M110.166108

Ryuichi Sugiyama[‡], Hironori Nishitsuji[‡], Ayako Furukawa[§], Masato Katahira[§1], Yuichiro Habu[¶], Hiroaki Takeuchi[‖], Akihide Ryo[**], and Hiroshi Takaku[‡2]

From the [‡]Department of Life and Environmental Sciences, Chiba Institute of Technology, 2-17-1 Tsudanuma, Narashino, Chiba 275-0016, Japan, the [§]Institute of Advanced Energy, Kyoto University, Gokasho, Uji, Kyoto 611-0011, Japan, the [¶]Department of Microbiology, Immunology, and Pathology, Colorado State University, Fort Collins, Colorado 80523-1619, the [‖]International Research Center for Infectious Diseases, The Institute of Medical Science, The University of Tokyo, 4-6-1 Shirokanedai, Minato-ku, Tokyo 108-8639, Japan, and the [**]Department of Microbiology, Yokohama City University School of Medicine, 3-9 Fukuura, Kanazawa-ku, Yokohama 236-0004, Japan

The cytidine deaminase APOBEC3G, which is incorporated into nascent virus particles, possesses potent antiviral activity and restricts Vif-deficient HIV-1 replication at the reverse transcription step through deamination-dependent and -independent effects. HIV-1 Vif counteracts the antiviral activity of APOBEC3G by inducing APOBEC3G polyubiquitination and its subsequent proteasomal degradation. In this study, we show that overexpression of heat shock protein 70 (HSP70) blocked the degradation of APOBEC3G in the ubiquitin-proteasome pathway by HIV-1 Vif, rendering the viral particles non-infectious. In addition, siRNA targeted knock-down of HSP70 expression enhanced the Vif-mediated degradation of APOBEC3G. A co-immunoprecipitation study revealed that overexpression of HSP70 inhibited APOBEC3G binding to HIV-1 Vif. Thus, we provide evidence for a host protein-mediated suppression of HIV-1 replication in an APOBEC3G-dependent manner.

Human immunodeficiency virus type-1 (HIV-1),[3] the retrovirus that causes AIDS, efficiently replicates within human $CD4^+$ T cells. However, Vif-deficient virions produced by non-permissive cells, including $CD4^+$ T cells and immortalized lines, such as Hut78 or CEM, are non-infections, whereas virions produced in permissive cells, such as SupT1 or CEM-SS, are infectious (1, 2). Previous studies have demonstrated that HIV-1 Vif counteracts the innate antiviral activity of APOBEC3G, a member of the APOBEC family of cytidine deaminase-editing enzymes (3). In the absence of Vif, APOBEC3G induces the deamination of cytidine (C) and its conversion to uridine (U) (4, 5), which can be packaged into budding retroviruses through a direct interaction with the Gag polyprotein (6–11). The C to U conversion in the HIV-1 minus strand leads to a G to A hypermutation, preferentially at CCCA sequences. This motif corresponds to TGGG in the plus-strand sequence, thereby mutating the TGG tryptophan codon to a TAG stop codon and affecting subsequent stages of the viral life cycle (12). Vif predominant mechanism for overcoming the antiviral activity of APOBEC3G is to form an E3 ubiquitin ligase with cullin 5 (Cul5), elongin B (EloB), and elongin C (EloC) and target these proteins for degradation by the ubiquitin-proteasome pathway (13–16). Vif may also inhibit APOBEC3G activity through mechanisms independent of proteasomal degradation (17–19).

Heat shock proteins play critical roles in the life cycle of a variety of RNA and DNA viruses (20–23). For example, heat shock protein 70 (HSP70) is specifically incorporated into HIV-1 virions (24). However, the formation of the P-TEFb/Tat/TAR complex is required to stabilize the CDK9/cyclinT1 heterodimer by HSP70 and HSP90 (25).

To better develop potential novel therapeutic strategies to exploit the APOBEC3G antiviral function, we investigated the role of HSP70 in APOBEC3G function. We found that siRNA against HSP70 significantly reduced the level of APOBEC3G in the presence of HIV-1 Vif, but not in the absence of Vif. In addition, overexpression of HSP70 in 293T cells reduced the Vif-mediated degradation of APOBEC3G by inhibiting APOBEC3G polyubiquitination. This effect is attributed to the impairment of APOBEC3G-Vif binding. Furthermore, overexpression of HSP70 in the presence, but not in the absence, of APOBEC3G clearly suppressed the infectivity of virions in a dose-dependent manner. These results suggest that HSP70 acts as a potential antiviral host factor through interaction with APOBEC3G and may form the basis for new anti-HIV-1 therapies.

EXPERIMENTAL PROCEDURES

Immunoprecipitation—293T cells (5×10^5) were transfected with 1.0 μg of each Vif expression plasmid using Lipofectamine2000 (Invitrogen). At 48 h post-transfection, cells were suspended in a lysis buffer (50 mM Tris-HCl, pH 7.0, 150 mM NaCl, 1% Nonidet P-40, and 10% glycerol) and incubated with 5 μl of anti-HSP70 antibody (Santa Cruz Biotechnology) and 30 μl of Dynabeads-protein G (Invitrogen). The beads were

* This work was supported in part by a Grant-in-aid for High Technology Research (No. 09309011) from the Ministry of Education, Science, Sports, and Culture of Japan and by a grant-in-aid for AIDS research from the Ministry of Health, Labor, and Welfare, Japan.
[1] Supported by Grants from MEXT (21370047 & 22121517), JST-SENTAN, Naito Foundation, and YCU-AMRC.
[2] To whom correspondence should be addressed: 2-17-1 Tsudanuma, Narashino, Chiba 275-0016, Japan. Tel.: 81-47-478-0407; Fax: 81-47-471-8764; E-mail: hiroshi.takaku@it-chiba.ac.jp.
[3] The abbreviations used are: HIV-1, human immunodeficiency virus type-1; RNP, ribonucleoprotein; HSP, heat shock protein; Ub, ubiquitin.

washed with PBS containing 0.02% Tween 20. The immunocomplex was eluted by boiling with 20 μl of 5× sample buffer and analyzed by SDS-PAGE and Western blot.

Protein Stability Assay—293T cells (5×10^5) were co-transfected with 1.0 μg of pc-Hu-APOBEC3G-HA and 0.5 μg of a GFP expression plasmid (CS-CDF-CG-PRE), or 1.0 μg of pc-Hu-APOBEC3G-HA, 0.5 μg of CS-CDF-CG-PRE and 0.5 μg of pcDNA-Vif along with either 2.0 μg of pFLAG-HSP70 or an empty plasmid. At 24 h post-transfection, cells were treated with 100 μg/ml of cycloheximide. Cells were harvested, and cell lysates were analyzed by Western blotting with horseradish peroxidase-conjugated anti-HA antibody (Roche Diagnostics) and anti-GFP antibody (Medical & Biological Laboratories). The blots were semi-quantified using ImageJ 1.43u software.

Polyubiquitination Assay—293T cells (3×10^6) were co-transfected with 2.0 μg of pc-Hu-APOBEC3G-HA, 2.0 μg of pVif-V5, 4.0 μg of pFLAG-HSP70, and 2.0 μg of pCMV-Myc-Ubi (26). At 24 h post-transfection, cells were treated with 5 μM MG-132 for 24 h. Cells were suspended in a lysis buffer. Cell lysates were immunoprecipitated using anti-Myc antibody (Cell Signaling) followed by Western blotting with horseradish peroxidase-conjugated anti-HA antibody.

MAGI Assay—MAGI cells were plated in 96-well plates at 1×10^4 cells per well in Dulbecco's modified Eagle's medium with 10% fetal bovine serum. The next day, cells were infected with dilutions of the virus in a total volume of 50 μl in the presence of 20 μg/ml DEAE-dextran for 2 h. At 2 days post-infection, cells were fixed with 100 μl of fix solution (1% formaldehyde/0.2% glutaraldehyde in PBS) at room temperature for 5 min and then washed twice with PBS. Cells were incubated with 100 μl of staining solution (4 mM potassium ferrocyanide, 4 mM potassium ferricyanide, 2 mM $MgCl_2$, and 0.4 mg/ml X-Gal) for 50 min at 37 °C. The reaction was stopped by removing the staining solution, and blue cells were counted under a microscope.

Construction of Plasmids—To generate pcDNA-Vif, HIV-1 Vif fragments were amplified from pNL4-3 by PCR with the following primers: forward 5′-GAT ATC ATG GAA AAC AGA TGG CAG GTG ATG-3′ and reverse 5′-CTC GAG CTA GTG TCC ATT CAT TGT ATG CT-3′. The PCR products were inserted into pcDNA3.1 (Invitrogen).

To construct pFLAG-HSP70, whole RNA was isolated from 293T cells with TRIzol (Invitrogen) and amplified by RT-PCR with the following primers: forward 5′-GTT GAA TTC CGC CAA AGC CGC GGC GAT-3′ and reverse 5′-CGC GGA TCC CTA ATC TAC CTC CTC AAT-3′. The products were inserted into pFLAG-CMV2 (Sigma).

To generate pVif-V5, HIV-1 Vif fragments were amplified from pNL4-3. The PCR products were inserted into pENTR using TOPO Cloning kits (Invitrogen) and transferred into pLenti6/V5-DEST (Invitrogen) by LR recombination. This construct contains the β-globin intron sequence of pMDL-g/p-RRE downstream of the CMV promoter. A plasmid construct encoding human APOBEC3G tagged with the influenza hemagglutinin (HA) sequence was a kind gift from Darlene Chen (The Salk Institute for Biological Studies). Vif-defective variants of NL4-3 have been described previously (27).

To generate pCS-U6, the U6 promoter was amplified by PCR. The resulting products were inserted into pCS-CDF-CG-PRE. pCS-U6-shControl or pCS-U6-shHSP70 was constructed by ligating the annealed product of sense oligonucleotide 5′-GAT CCT TCT CCG AAC GTG TCA CGT TTC AAG AGA ACG TGA CAC GTT CGG AGA ATT T-3′ and antisense oligonucleotide 5′-CTA GAA ATT CTC CGA ACG TGT CAC GTT CTC TTG AAA CGT GAC ACG TTC GGA GAA G-3′ or sense oligonucleotide 5′-GAT CCC ACG GCA AGG TGG AGA TCA TTC AAG AGA TGA TCT CCA CCT TGC CGT GTT T-3′ and antisense oligonucleotide 5′-CTA GAA ACA CGG CAA GGT GGA GAT CAT CTC TTG AAT GAT CTC CAC CTT GCC GTG G-3′, respectively, with the BamHI-XbaI fragment from pCS-U6. These plasmids contain a transcriptional termination signal sequence downstream of the shControl and shHSP70 sequences.

Transfection of siRNA—293T cells (3×10^6) were transfected with siRNAs (100 nM) using Lipofectamine2000. Control siRNA (5′-UUC UCC GAA CGU GUC ACG UdTdT-3′) and HSP70-siRNA (5′-CAC GGC AAG GUG GAG AUC AdTdT-3′) were purchased from B-Bridge International.

Preparation of Lentiviral Vectors—293T cells (5×10^5) were cotransfected with the lentiviral vector (1.6 μg), vesicular stomatitis virus G expression vector pMD.G (0.4 μg), *rev* expression vector pRSV-Rev (0.8 μg), and *gag-pol* expression vector pMDLg/pRRE (1.2 μg) using Lipofectamine2000. At 48 h after transfection, culture supernatants were harvested and filtered through 0.45-μm filters. In all experiments, H9 cells (3×10^5) were transduced with equal amounts of the lentivirus vector.

Statistical Analysis—The results are shown as means ± S.D., and statistical analysis was performed using the paired Student's *t* test. A p value of <0.05 was considered significant. At least three replicates were performed for each experiment.

RESULTS

HSP70 Leads to Stabilization of APOBEC3G—HSPs are induced by a variety of stress-related stimuli, including heat, UV radiation, and microbial/viral infections (28). HSPs are involved in the folding and translocation of cellular proteins under normal conditions, whereas under stressful conditions, HSPs bind to proteins and inhibit their misfolding or irreversible aggregation (29). Recent studies revealed that the binding of HSPs to HIV-1 proteins enhances antiviral immunity (30). HSP70 is selectively expressed soon after HIV-1 infection, suggesting that these proteins might be involved in the innate cellular antiviral immune response (31). However, the specific targets of HSPs and their role in the response to HIV infection remain unclear.

HIV-1 Vif targets APOBEC3G for ubiquitination by forming an Skp1-cullin-F-box (SCF)-like complex, which subsequently leads to the degradation of APOBEC3G. To evaluate how HSP70 affects Vif-dependent ubiquitination and degradation, we examined the steady-state level of APOBEC3G in 293T cells co-transfected with FLAG-tagged HSP70 (FLAG-HSP70) and pNL4-3. The expression of HSP70 in 293T cells significantly increased the amount of APOBEC3G in a dose-dependent manner but not the amount of the HIV-1 Gag p24 antigen (Fig. 1*A*, *lanes 1–4* and Fig. 1*B*). Importantly, HSP70 had no effect on

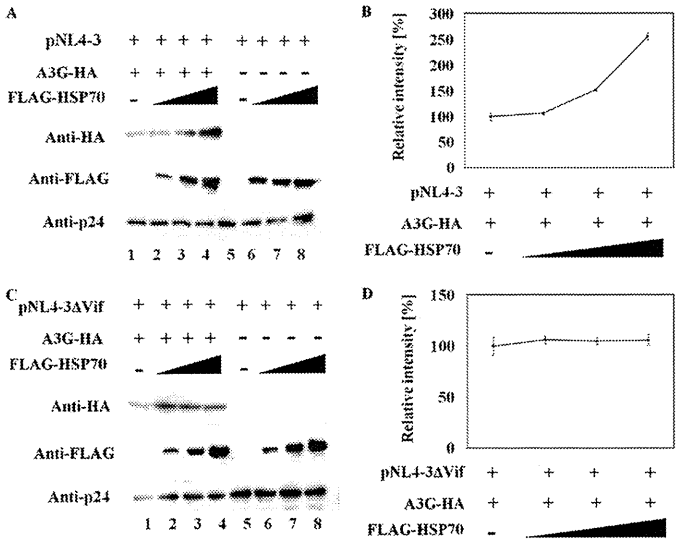

FIGURE 1. **Expression of FLAG-tagged HSP70 blocks APOBEC3G degradation in cells transfected with pNL4-3, but not those transfected with pNL4-3-delta-Vif.** 293T cells (5×10^5) were co-transfected with 1.0 μg of pc-Hu-APOBEC3G-HA and increasing amounts of pFLAG-HSP70 (0, 0.5, 1.0, or 2.0 μg), adjusted with an empty vector to 2.0 μg of total, along with either 0.1 μg of pNL4-3 (*A*) or 0.1 μg of pNL4-3-delta-Vif (*C*). At 48 h post-transfection, cell lysates were analyzed by Western blotting. The relative intensity of APOBEC3G-HA bands was determined by densitometry (*B* and *D*). Results are representative of three independent experiments, and error bars show the standard deviations of the means.

the expression level of APOBEC3G in 293T cells transfected with Vif-deleted HIV-1 proviral plasmid (Fig. 1, *C*, *lanes 1–4* and *D*). Our results suggest that HSP70 may inhibit the degradation of APOBEC3G by HIV-1 Vif.

HSP70 Blocks HIV-1 Vif-mediated Degradation of APOBEC3G—Next, we investigated whether expression of HSP70 directly blocks APOBEC3G degradation by HIV-1 Vif. 293T cells were co-transfected with pc-Hu-APOBEC3G-HA and pFLAG-HSP70 in the absence or presence of pcDNA-Vif. We found that the steady-state levels of APOBEC3G in the presence of pcDNA-Vif were increased by the expression of HSP70 in a dose-dependent manner (Fig. 2, *A*, *lanes 6–10* and *B*, *right panel*). By contrast, HSP70 did not significantly affect the amount of APOBEC3G expression in the absence of pcDNA-Vif (Fig. 2, *A*, *lanes 1–5* and *B*, *left panel*). These data indicate that the effects of HSP70 on APOBEC3G expression depend on HIV-1 Vif.

Previous studies have reported that microbial HSP70 up-regulates APOBEC3G mRNA (32, 33). To rule out this possibility, pulse-chase experiments were performed using 293T cells that were co-transfected with pc-Hu-APOBEC3G-HA, pVif-V5, pFLAG-HSP70, and a GFP expression plasmid (CS-CDF-CG-PRE). Cycloheximide was used to block protein synthesis. When 293T cells were transfected with pc-Hu-APOBEC3G-HA alone, there was no change in the level of APOBEC3G (Fig. 2, *C*, *lanes 1–4* and *D*, *left panel*). Consistent with previous reports, degradation of APOBEC3G-HA was induced in the presence of HIV-1 Vif (Fig. 2, *C*, *lanes 5–8* and *D*, *middle panel*). In contrast, HSP70 expression significantly suppressed the degradation of APOBEC3G by HIV-1 Vif (Fig. 2, *C*, *lanes 9–12* and *D*, *right panel*). To further evaluate whether HSP70 expression inhibits the ubiquitination of APOBEC3G by HIV-1 Vif, we performed ubiquitination assays. Lysates of cells co-expressing pVif-V5, Myc-tagged ubiquitin (Myc-Ub), pc-Hu-APOBEC3G-HA and either empty plasmid or pFLAG-HSP70 were analyzed for the polyubiquitination of APOBEC3G. We detected the ubiquitination of APOBEC3G as a ladder band (Fig. 2*E*, *lane 2*). The expression of HSP70 resulted in a significant reduction in polyubiquitinated APOBEC3G (Fig. 2*E*, *lane 1*). Thus, the expression of HSP70 causes an increase in the steady-state levels of APOBEC3G by blocking the Vif-mediated ubiquitination and degradation of APOBEC3G.

HSP70 Interacts with Both APOBEC3G and HIV-1 Vif—We performed an immunoprecipitation assay to evaluate the binding between HSP70 and APOBEC3G or HIV-1 Vif (Fig. 3). 293T cells were transfected with pc-Hu-APOBEC3G-HA, pcDNA-Vif, pNL4-3, or pNL4-3-delta-Vif. Cell lysates were precipitated with anti-HSP70 antibody, followed by immunoblotting with anti-ApoC17 or anti-Vif antibody. HSP70 interacted with both APOBEC3G (Fig. 3*A*) and HIV-1 Vif (Fig. 3*B*). These interactions and the intracellular localization of HSP70 and HA-tagged APOBEC3G were confirmed by immunostaining assays (data not shown). To further investigate the role of HSP70 in APOBEC3G-Vif interactions, 293T cells were co-transfected with pc-Hu-APOBEC3G-HA and pVif-V5 along with either an empty plasmid or pFLAG-HSP70 in the presence of a proteasome inhibitor (MG-132). Consistent with previous studies, HIV-1 Vif was bound to APOBEC3G (Fig. 3*C*, *lane 2*). Strikingly, the expression of HSP70 in 293T cells led to the inhibition of APOBEC3G-Vif binding. (Fig. 3*C*, *lane 1*). Because a previous study reported that APOBEC3G binds the N-terminal region of HIV-1 Vif (34), we tested the hypothesis that HSP70 competes with APOBEC3G for binding to the N-terminal region of HIV-1 Vif. We found that FLAG-HSP70 efficiently co-immunoprecipitated with the N-terminal region of Vif (amino acids 1–107) (Fig. 3*D*, *lane 1*). However, the C-terminal region of Vif (amino acids 108–192) exhibited no detectable interaction with FLAG-HSP70 (Fig. 3*D*, *lane 2*). These results suggest that APOBEC3G-Vif binding is reduced by HSP70 through an interaction with the N-terminal region of Vif, resulting in the inhibition of the Vif-mediated ubiquitination and the degradation of APOBEC3G.

Knock-down of HSP70 in 293T Cells Enhances APOBEC3G Degradation by HIV-1 Vif—To further investigate the effect of endogenous HSP70 on the stability of APOBEC3G, we silenced endogenous HSP70 expression by RNA interference. 293T cells were transfected with control siRNA (siCtrl) or HSP70-specific siRNA (siHSP70) for 4 h prior to transfection along with pc-Hu-APOBEC3G-HA and either pNL4-3 or pNL4-3-delta-Vif. At 48 h post-transfection, cells were harvested and subjected to Western blotting. As expected, the level of APOBEC3G in pNL4-3-transfected cells was less stable than that in the pNL4-3-delta-Vif transfected cells (Fig. 4*A*, compare *lane 1* to *lane 3*). Quantification of the relative intensities revealed that transfection with pNL4-3 induced APOBEC3G degradation with a potency ~1.8 times higher than that of pNL4-3-delta-Vif (Fig. 4*B*). Moreover, in the case of transfection with pNL4-3, the level of APOBEC3G, but not the level of HIV-1 Gag, in the siHSP70-transduced cells were lower than in

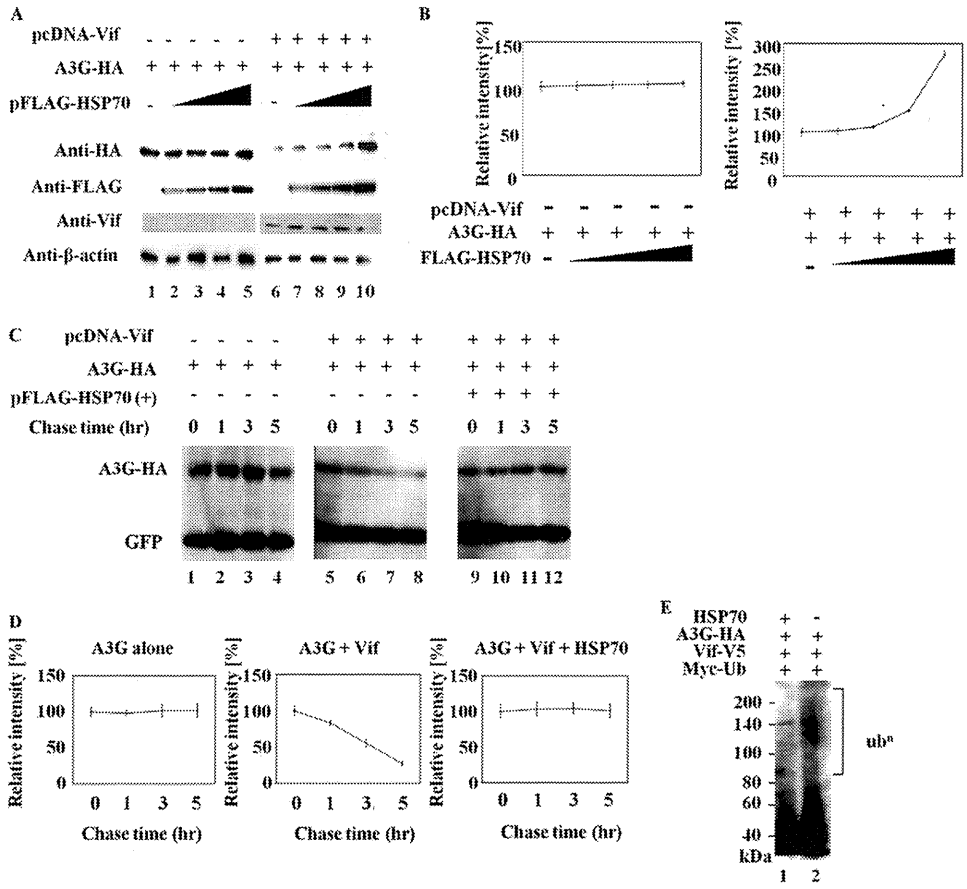

FIGURE 2. **HSP70 expression inhibits Vif-mediated APOBEC3G ubiquitination and degradation.** *A*, 293T cells (5×10^5) were co-transfected with 1.0 μg of pc-Hu-APOBEC3G-HA and increasing amounts of pFLAG-HSP70 (0, 0.5, 1.0, or 2.0 μg), adjusted to 2.0 μg of total DNA with 0.5 μg of an empty plasmid (pcDNA3.1) or pcDNA-Vif. At 48 h post-transfection, cell lysates were subjected to Western blotting and were then analyzed with the indicated antibody. β-Actin was used as a control for protein levels. *B*, relative intensity of APOBEC3G-HA bands in *A* was determined by densitometry. *C*, 293T cells (5×10^5) were transfected with 1.0 μg of pc-Hu-APOBEC3G-HA alone (*lanes 1–4*); 0.5 μg of pcDNA-Vif and 1.0 μg of pc-Hu-APOBEC3G-HA (*lanes 5–8*); and 0.5 μg of pcDNA-Vif, 1.0 μg of pc-Hu-APOBEC3G-HA and 2.0 μg of pFLAG-HSP70 (*lanes 9–12*). The transfected cells were treated with cycloheximide to block *de novo* protein synthesis. The level of APOBEC3G was detected by immunoblotting after cycloheximide treatment lasting 1, 3, or 5 h. CS-CDF-CG-PRE (0.5 μg), which expresses the green fluorescent protein (GFP), was co-transfected with each plasmid into 293T cells as a control plasmid. *D*, relative intensity of APOBEC3G-HA bands in *C* was determined by densitometry. *E*, 293T cells (3×10^6) were co-transfected with 2.0 μg of pCMV-Myc-Ubi, 2.0 μg of pVif-V5, and 2.0 μg of pc-Hu-APOBEC3G-HA along with 4.0 μg of an empty plasmid or pFLAG-HSP70. At 24 h post-transfection, cells were treated with 5 μM MG132. After 24 h, cell lysates were immunoprecipitated with anti-Myc antibody, followed by immunoblotting analysis with horseradish peroxidase-conjugated anti-HA antibody. Results are representative of three independent experiments, and error bars show the standard deviations of the means.

the siCtrl-transduced cells (Fig. 4*A*, compare *lane 1* to *lane 2*). The amount of APOBEC3G in HSP70 knock-down cells decreased to half the amount in the control cells (Fig. 4*B*). However, in terms of transfection with pNL4-3-delta-Vif, treatment with siHSP70 had no effect on the stability of APOBEC3G (Fig. 4*A*, compare *lane 3* to *lane 4*). These data indicate that depletion of HSP70 facilitates Vif-mediated degradation of APOBEC3G.

HSP70 Suppresses HIV-1 Vif-mediated Degradation of Endogenous APOBEC3G in Non-permissive Cells—Most experiments in this study used permissive cells. To investigate whether our findings have physiologic relevance in non-permissive cells, we used a lentiviral vector encoding FLAG-HSP70 or HIV-1 Vif-V5. In the absence of Vif-V5, there was no significant effect of FLAG-HSP70 on the level of endogenous APOBEC3G in H9 cells (Fig. 5*A*, compare *lane 1* to *lane 2*). When Vif-V5 was expressed in H9 cells, expression of FLAG-HSP70 increased the amount of endogenous APOBEC3G (Fig. 5*A*, compare *lane 3* to *lane 4*). Next, we suppressed the expression of HSP70 using a lentiviral vector to express shHSP70 under the control of the human U6 promoter in H9 cells. APOBEC3G expression in shHSP70-transduced H9 cells was similar to that in shControl-transduced H9 cells (Fig. 5*B*, compare *lane 1* to *lane 2*). The level of endogenous APOBEC3G was lower in H9 cells transduced with shHSP70 than in H9 cells transduced with shControl by expression of Vif-V5 (Fig. 5*B*, compare *lane 3* to *lane 4*). Therefore, HSP70 suppresses Vif-mediated degradation of endogenous APOBEC3G in non-permissive cells.

Expression of HSP70 in the Presence of APOBEC3G Augments APOBEC3G Restriction of HIV-1—To examine whether HSP70 expression influences the function of APOBEC3G, pNL4-3, or pNL4-3-delta-Vif was transfected into 293T cells along with either pFLAG-HSP70 alone or pFLAG-HSP70 and pc-Hu-APOBEC3G-HA. The viral infectivity was measured by MAGI assay. As shown in Fig. 6*A*, expression of FLAG-HSP70 clearly suppressed the infectivity of wild-type HIV-1 in the presence of APOBEC3G in a dose-dependent manner. In the absence of APOBEC3G, FLAG-HSP70 did not affect the infectivity of the wild-type HIV-1. Unexpectedly, HSP70 expression in

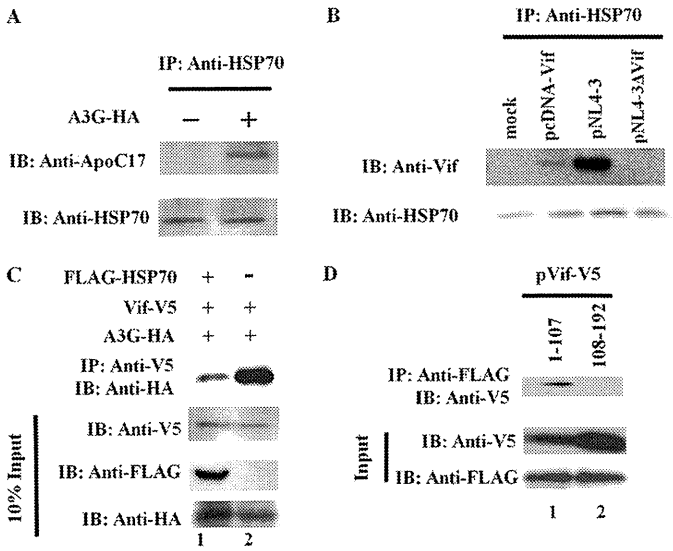

FIGURE 3. **HSP70 interacts with APOBEC3G and HIV-1 Vif.** *A*, 293T cells (5×10^5) were transfected with 1.0 μg of pc-Hu-APOBEC3G-HA. After 48 h, cell lysates were immunoprecipitated with anti-HSP70 antibody, followed by immunoblotting analysis with anti-ApoC17 antibody. *B*, 293T cells (5×10^5) were transfected with 1.0 μg of the indicated plasmids. At 48 h post-transfection, cell lysates were subjected to immunoprecipitation using anti-HSP70 antibody, followed by immunoblotting analysis with anti-Vif antibody. *C*, 293T cells (5×10^5) were co-transfected with 1.0 μg of pc-Hu-APOBEC3G-HA and 1.0 μg of pVif-V5 together with 2.0 μg of either an empty plasmid or pFLAG-HSP70. At 24 h post-transfection, cells were treated with 5 μM MG132. At 24 h post-treatment, cell lysates were immunoprecipitated with anti-V5 antibody, followed by immunoblotting analysis with horseradish peroxidase-conjugated anti-HA antibody. *D*, 293T cells (5×10^5) were co-transfected with 1.0 μg of pFLAG-HSP70 and either 1.0 μg of pVif-1–107-V5 or pVif-108–192-V5. At 48 h post-transfection, cell lysates were immunoprecipitated with anti-FLAG antibody, followed by immunoblotting analysis with anti-V5 antibody. Results are representative of three independent experiments.

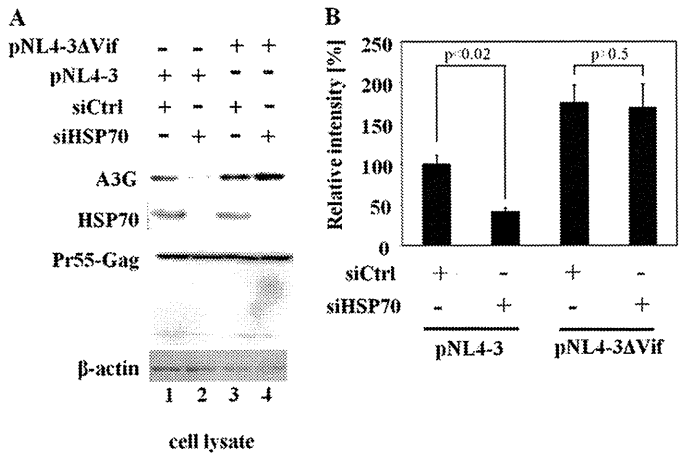

FIGURE 4. **Depletion of HSP70 in 293T cells impairs the stability of APOBEC3G.** *A*, 293T cells (3×10^6) were treated with 100 nM HSP70-siRNA (siHSP70) or 100 nM control-siRNA (siCtrl) for 4 h, prior to co-transfection with 1.0 μg of pc-Hu-APOBEC3G-HA with either 1.0 μg of pNL4-3 or pNL4-3-delta-Vif. At 48 h post-transfection, cell lysates were analyzed by Western blotting using the indicated antibodies. *B*, relative intensity of APOBEC3G bands in *A* was determined by densitometry. Results are representative of three independent experiments, and error bars show the standard deviations of the means.

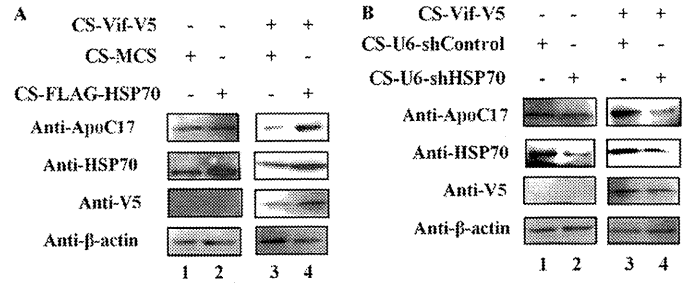

FIGURE 5. **HSP70 affects the level of endogenous APOBEC3G expression in non-permissive T cells expressing HIV-1 Vif.** *A*, H9 cells (3×10^5) were infected with a lentiviral vector encoding an artificial multiple cloning site (MCS) or FLAG-HSP70 in the presence of 8 μg/ml of polybrene. At 48 h after infection, cells were suspended with lysis buffer (*left panel*) or transduced with HIV-1 Vif using a lentivirus vector system (*right panel*). At 48 h post-transduction, cell lysates were analyzed by Western blotting using the indicated antibodies. *B*, H9 cells (3×10^5) were infected with lentivirus-based vectors to express shControl or shHSP70 under the control of the human U6 promoter in the presence of 8 μg/ml of polybrene. At 48 h post-infection, cells were treated as in *A*. Data are representative of three independent experiments.

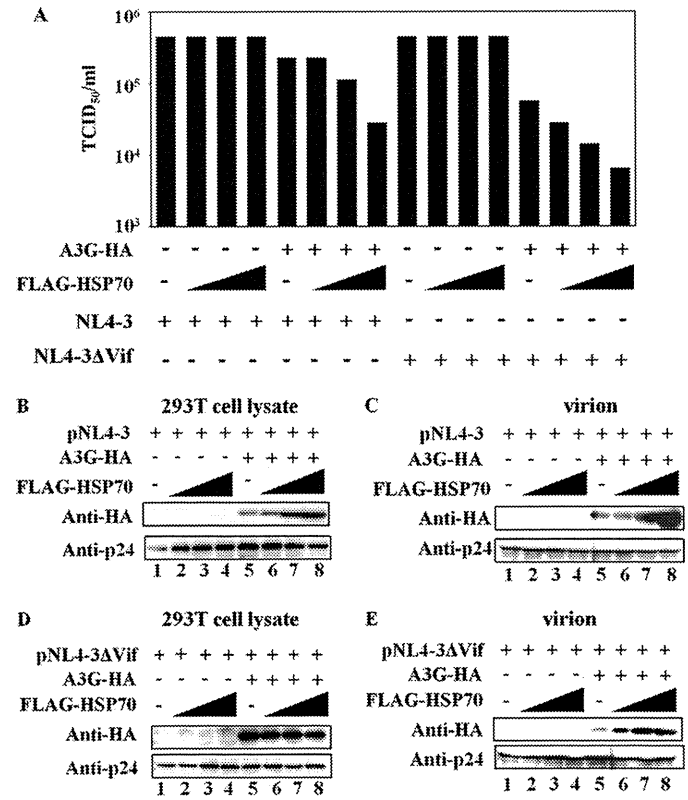

FIGURE 6. **HSP70 regulates HIV-1 infectivity in an APOBEC3G-dependent manner.** *A*, 293T cells (5×10^5) were co-transfected with 0.1 μg of pNL4-3 or pNL4-3-delta-Vif and 1.0 μg of pc-Hu-APOBEC3G-HA alone, pFLAG-HSP70 (0.5, 1.0, or 2.0 μg) alone or 1.0 μg of pc-Hu-APOBEC3G-HA and pFLAG-HSP70 (0.5, 1.0 or 2.0 μg). At 48 h post-transfection, supernatants were harvested, and the amount of each virus was normalized to the equivalent level of p24. MAGI cells (1×10^4) were infected with serially diluting supernatants of each stock of virus, and infected cells were stained with X-Gal 2 days later. 50% tissue culture infective doses (TCID50) is determined by the last virus dilution that is still capable of infecting the cells. *B*, each stock of cell lysate or virus in *A* was subjected to Western blotting and was then analyzed with the indicated antibody. All data are representative of three independent experiments.

APOBEC3G-HA-transfected 293T cells led to a dose-dependent inhibition of the infectivity of Vif-deficient HIV-1 particles (Fig. 6*A*). Moreover, no effect of HSP70 expression on the infectivity of the Vif-deficient HIV-1 particles produced by mock-transfected 293T cells was observed. To further demonstrate whether expression of HSP70 affects virion packaging of APOBEC3G, viral particles produced by 293T cells expressing

HSP70 were analyzed for APOBEC3G expression by Western blotting. We found that expression of HSP70 significantly increased the amount of intracellular and wild type virion-associated APOBEC3G (Fig. 6, *B* and *C*). Interestingly, HSP70 expression enhanced the level of APOBEC3G packaging in Vif-deficient virions, but had no effect on intracellular APOBEC3G and viral release (Fig. 6, *D* and *E*). These results indicate that HSP70 blocks Vif-mediated APOBEC3G degradation and enhances the incorporation of APOBEC3G into both wild type and Vif-deficient virions, which result from inhibition of HIV-1 replication through HSP70 interaction with APOBEC3G.

DISCUSSION

APOBEC3G, which is incorporated into progeny virus particles, restricts the replication of Vif-deficient HIV-1 through cytidine deamination-dependent and independent mechanisms (3–5, 17, 35–41). This restriction can be overcome by HIV-1 Vif, which induces the polyubiquitination of APOBEC3G through recruitment of a ubiquitin E3 ligase complex composed of cullin 5, elongin B, elongin C, and Ring box-1 and facilitates the proteasomal degradation of APOBEC3G (13, 14, 16, 42–45). Thus, mechanistic insights into the quality control of APOBEC3G protein are important for understanding the molecular basis of APOBEC3G-mediated HIV-1 restriction. In this study, we showed that HSP70 suppressed Vif-mediated APOBEC3G degradation. In contrast to our results for HSP70, Pin1 suppresses the HIV restriction activity of APOBEC3G (46). Overexpression of Pin1 reduces the levels of intracellular APOBEC3G. One possibility is that HSP70 regulates Pin1 function, which results in the stimulation of APOBEC3G function, although further analysis is needed to properly address this question.

Pido-Lopez *et al.* (32) have reported that microbial HSP70 up-regulates APOBEC3G mRNA and protein expression in human $CD4^+$ T cells. Our data indicate that in 293T cells, overexpression of human HSP70 in the absence of HIV-1 Vif did not affect the amount of APOBEC3G protein. The stabilization of APOBEC3G is attributed to a reduction in the Vif-dependent polyubiquitination of APOBEC3G (Fig. 2*E*). Whereas we have focused on human HSP70 activity on APOBEC3G stability, it would be interesting to investigate whether human HSP70 can affect the level of endogenous APOBEC3G mRNA.

APOBEC3G associates with ribonucleoprotein (RNP) complexes and is not only dispersed throughout the cytoplasm but is also markedly concentrated in cytoplasmic foci that are identified as mRNA-processing bodies (P bodies) (47). Localization of APOBEC3G in P bodies is not important for its LINE-1 suppression activity (48). However, Y3 and 7SL RNAs, which compose RNP complexes, are required for efficient APOBEC3G packaging (49). Stimulation of cells at 44 °C induces the rapid accumulation of APOBEC3G and many cellular RNA-binding proteins (50). We examined whether HSP70 plays a role in packaging APOBEC3G into virus particles and found that overexpression of HSP70 enhanced APOBEC3G packaging in the absence of Vif (Fig. 6*E*). It is possible that HSP70 interacts with cytoplasmic APOBEC3G, but it remains unclear whether HSP70 induces the accumulation of APOBEC3G in P bodies and increases the association of APOBEC3G with RNP complexes. Further studies will be required to clarify the details of how, where and when HSP70 and APOBEC3G co-localize within cells.

Recently, Nathans *et al.* (51) have identified a small molecule, termed RN-18, that degrades HIV-1 Vif only in the presence of APOBEC3G, resulting in enhanced APOBEC3G abundance and virion incorporation, similar to the function of HSP70. The possibility has been raised that HSP70 may be the target of RN-18. However, HSP70 has no significant effect on HIV-1 Vif expression and leads to the increase of APOBEC3G packaging into virions in a Vif-independent manner. Moreover, RN-18 exhibits a strong dependence on APOBEC3G, whereas HSP70 can interact directly with both HIV-1 Vif and APOBEC3G. Thus, RN-18 probably does not target HSP70. Taken together, the results of the present study suggest that stimulation of innate immunity, such as that mediated by APOBEC3G, may aid in the development of antiviral therapies.

Acknowledgments—We thank Dr. Darlene Chen for providing pc-Hu-APOBEC3G-HA, Dr. Miyoshi Hiroyuki for providing pCS-CDF-CG-PRE, and Haruki Naganuma and Hiroshi Koseki for technical assistance.

REFERENCES

1. Gabuzda, D. H., Lawrence, K., Langhoff, E., Terwilliger, E., Dorfman, T., Haseltine, W. A., and Sodroski, J. (1992) *J. Virol.* **66,** 6489–6495
2. von Schwedler, U., Song, J., Aiken, C., and Trono, D. (1993) *J. Virol.* **67,** 4945–4955
3. Sheehy, A. M., Gaddis, N. C., Choi, J. D., and Malim, M. H. (2002) *Nature* **418,** 646–650
4. Zhang, H., Yang, B., Pomerantz, R. J., Zhang, C., Arunachalam, S. C., and Gao, L. (2003) *Nature* **424,** 94–98
5. Harris, R. S., Bishop, K. N., Sheehy, A. M., Craig, H. M., Petersen-Mahrt, S. K., Watt, I. N., Neuberger, M. S., and Malim, M. H. (2003) *Cell* **113,** 803–809
6. Cen, S., Guo, F., Niu, M., Saadatmand, J., Deflassieux, J., and Kleiman, L. (2004) *J. Biol. Chem.* **279,** 33177–33184
7. Svarovskaia, E. S., Xu, H., Mbisa, J. L., Barr, R., Gorelick, R. J., Ono, A., Freed, E. O., Hu, W. S., and Pathak, V. K. (2004) *J. Biol. Chem.* **279,** 35822–35828
8. Alce, T. M., and Popik, W. (2004) *J. Biol. Chem.* **279,** 34083–34086
9. Douaisi, M., Dussart, S., Courcoul, M., Bessou, G., Vigne, R., and Decroly, E. (2004) *Biochem. Biophys. Res. Commun.* **321,** 566–573
10. Schäfer, A., Bogerd, H. P., and Cullen, B. R. (2004) *Virology* **328,** 163–168
11. Kremer, M., Bittner, A., and Schnierle, B. S. (2005) *Virology* **337,** 175–182
12. Yu, Q., König, R., Pillai, S., Chiles, K., Kearney, M., Palmer, S., Richman, D., Coffin, J. M., and Landau, N. R. (2004) *Nat. Struct. Mol. Biol.* **11,** 435–442
13. Yu, X., Yu, Y., Liu, B., Luo, K., Kong, W., Mao, P., and Yu, X. F. (2003) *Science* **302,** 1056–1060
14. Mehle, A., Goncalves, J., Santa-Marta, M., McPike, M., and Gabuzda, D. (2004) *Genes Dev.* **18,** 2861–2866
15. Yu, Y., Xiao, Z., Ehrlich, E. S., Yu, X., and Yu, X. F. (2004) *Genes Dev.* **18,** 2867–2872
16. Kobayashi, M., Takaori-Kondo, A., Miyauchi, Y., Iwai, K., and Uchiyama, T. (2005) *J. Biol. Chem.* **280,** 18573–18578
17. Iwatani, Y., Chan, D. S., Wang, F., Maynard, K. S., Sugiura, W., Gronenborn, A. M., Rouzina, I., Williams, M. C., Musier-Forsyth, K., and Levin, J. G. (2007) *Nucleic. Acids Res.* **35,** 7096–7108
18. Stopak, K., de Noronha, C., Yonemoto, W., and Greene, W. C. (2003) *Mol. Cell* **12,** 591–601
19. Mercenne, G., Bernacchi, S., Richer, D., Bec, G., Henriet, S., Paillart, J. C., and Marquet, R. (2010) *Nucleic. Acids Res.* **38,** 633–646
20. Parent, R., Qu, X., Petit, M. A., and Beretta, L. (2009) *Hepatology* **49,**

1798–1809
21. Padwad, Y. S., Mishra, K. P., Jain, M., Chanda, S., Karan, D., and Ganju, L. (2009) *Immunobiology* **214,** 422–429
22. Ujino, S., Yamaguchi, S., Shimotohno, K., and Takaku, H. (2009) *J. Biol. Chem.* **284,** 6841–6846
23. Chase, G., Deng, T., Fodor, E., Leung, B. W., Mayer, D., Schwemmle, M., and Brownlee, G. (2008) *Virology* **377,** 431–439
24. Gurer, C., Cimarelli, A., and Luban, J. (2002) *J. Virol.* **76,** 4666–4670
25. O'Keeffe, B., Fong, Y., Chen, D., Zhou, S., and Zhou, Q. (2000) *J. Biol. Chem.* **275,** 279–287
26. Ryo, A., Suizu, F., Yoshida, Y., Perrem, K., Liou, Y. C., Wulf, G., Rottapel, R., Yamaoka, S., and Lu, K. P. (2003) *Mol. Cell* **12,** 1413–1426
27. Karczewski, M. K., and Strebel, K. (1996) *J. Virol.* **70,** 494–507
28. Neidhardt, F. C., VanBogelen, R. A., and Vaughn, V. (1984) *Annu. Rev. Genet.* **18,** 295–329
29. Bukau, B., Weissman, J., and Horwich, A. (2006) *Cell* **125,** 443–451
30. SenGupta, D., Norris, P. J., Suscovich, T. J., Hassan-Zahraee, M., Moffett, H. F., Trocha, A., Draenert, R., Goulder, P. J., Binder, R. J., Levey, D. L., Walker, B. D., Srivastava, P. K., and Brander, C. (2004) *J. Immunol.* **173,** 1987–1993
31. Wainberg, Z., Oliveira, M., Lerner, S., Tao, Y., and Brenner, B. G. (1997) *Virology* **233,** 364–373
32. Pido-Lopez, J., Whittall, T., Wang, Y., Bergmeier, L. A., Babaahmady, K., Singh, M., and Lehner, T. (2007) *J. Immunol.* **178,** 1671–1679
33. Babaahmady, K., Oehlmann, W., Singh, M., and Lehner, T. (2007) *J. Virol.* **81,** 3354–3360
34. Mehle, A., Wilson, H., Zhang, C., Brazier, A. J., McPike, M., Pery, E., and Gabuzda, D. (2007) *J. Virol.* **81,** 13235–13241
35. Bishop, K. N., Holmes, R. K., and Malim, M. H. (2006) *J. Virol.* **80,** 8450–8458
36. Bishop, K. N., Verma, M., Kim, E. Y., Wolinsky, S. M., and Malim, M. H. (2008) *PLoS Pathog.* **4,** e1000231
37. Guo, F., Cen, S., Niu, M., Yang, Y., Gorelick, R. J., and Kleiman, L. (2007) *J. Virol.* **81,** 11322–11331
38. Lecossier, D., Bouchonnet, F., Clavel, F., and Hance, A. J. (2003) *Science* **300,** 1112
39. Li, X. Y., Guo, F., Zhang, L., Kleiman, L., and Cen, S. (2007) *J. Biol. Chem.* **282,** 32065–32074
40. Mangeat, B., Turelli, P., Caron, G., Friedli, M., Perrin, L., and Trono, D. (2003) *Nature* **424,** 99–103
41. Suspène, R., Sommer, P., Henry, M., Ferris, S., Guétard, D., Pochet, S., Chester, A., Navaratnam, N., Wain-Hobson, S., and Vartanian, J. P. (2004) *Nucleic. Acids Res.* **32,** 2421–2429
42. Sheehy, A. M., Gaddis, N. C., and Malim, M. H. (2003) *Nat. Med.* **9,** 1404–1407
43. Marin, M., Rose, K. M., Kozak, S. L., and Kabat, D. (2003) *Nat. Med.* **9,** 1398–1403
44. Conticello, S. G., Harris, R. S., and Neuberger, M. S. (2003) *Curr. Biol.* **13,** 2009–2013
45. Mehle, A., Strack, B., Ancuta, P., Zhang, C., McPike, M., and Gabuzda, D. (2004) *J. Biol. Chem.* **279,** 7792–7798
46. Watashi, K., Khan, M., Yedavalli, V. R., Yeung, M. L., Strebel, K., and Jeang, K. T. (2008) *J. Virol.* **82,** 9928–9936
47. Gallois-Montbrun, S., Kramer, B., Swanson, C. M., Byers, H., Lynham, S., Ward, M., and Malim, M. H. (2007) *J. Virol.* **81,** 2165–2178
48. Niewiadomska, A. M., Tian, C., Tan, L., Wang, T., Sarkis, P. T., and Yu, X. F. (2007) *J. Virol.* **81,** 9577–9583
49. Wang, T., Tian, C., Zhang, W., Luo, K., Sarkis, P. T., Yu, L., Liu, B., Yu, Y., and Yu, X. F. (2007) *J. Virol.* **81,** 13112–13124
50. Gallois-Montbrun, S., Holmes, R. K., Swanson, C. M., Fernández-Ocaña, M., Byers, H. L., Ward, M. A., and Malim, M. H. (2008) *J. Virol.* **82,** 5636–5642
51. Nathans, R., Cao, H., Sharova, N., Ali, A., Sharkey, M., Stranska, R., Stevenson, M., and Rana, T. M. (2008) *Nat. Biotechnol.* **26,** 1187–1192

FEBS Letters 585 (2011) 3372–3377

FEBS Letters

journal homepage: www.FEBSLetters.org

Identification of amino acid residues in HIV-1 reverse transcriptase that are critical for the proteolytic processing of Gag–Pol precursors

Hironori Nishitsuji [a,*], Masaru Yokoyama [c], Hironori Sato [c], Suguru Yamauchi [a], Hiroshi Takaku [a,b,*]

[a] Department of Life and Environmental Sciences, Chiba Institute of Technology, 2-17-1 Tsudanuma, Narashino, Chiba 275-0016, Japan
[b] High Technology Research Center, Chiba Institute of Technology, 2-17-1 Tsudanuma, Narashino, Chiba 275-0016, Japan
[c] Pathogen Genomics Center, National Institute of Infectious Diseases, 4-7-1 Gakuen, Musashi Murayama-shi, Tokyo 208-0011, Japan

ARTICLE INFO

Article history:
Received 1 July 2011
Revised 22 September 2011
Accepted 23 September 2011
Available online 12 October 2011

Edited by Ivan Sadowski

Keywords:
Human immunodeficiency virus type 1
Reverse transcriptase
Gag–Pol
Processing

ABSTRACT

The efficient processing of human immunodeficiency virus type 1 Gag–Pol requires not only protease activity but also specific reverse transcriptase (RT) and integrase sequences. However, the critical amino acid residues of the HIV-1 Pol gene involved in protease-mediated Gag–Pol processing have not been precisely defined. Here, we found that the substitution of Thr-128 or Tyr-146 with Ala markedly impaired the proteolytic processing of the MA/CA, p66/p51 and RT/IN sites but did not affect the normal processing of other sites. Moreover, a Thr-128 or Tyr-146 mutation in RT abolished RT dimerization in vitro. These results suggest that Thr-128 and Tyr-146 within the RT region play important roles in protease-mediated Gag–Pol processing.

Structured summary of protein interactions:
RT and **RT** physically interact by cross-linking study (View interaction: 1, 2, 3).
CK2 alpha phosphorylates RT by protein kinase assay (View interaction).

1. Introduction

The human immunodeficiency virus type 1 (HIV-1) Gag–Pol is normally translated by a −1 ribosomal frameshift event occurring at a frequency of approximately 5% during Gag translation, resulting in a 1:20 ratio of synthesized Gag–Pol to Pr55-Gag [1]. The incorporation of Gag–Pol into virus particles requires its interaction with Pr55-Gag [2]. The processing of Gag–Pol is accomplished by viral protease activation during Gag–Pol/Gag–Pol interactions or Gag–Pol multimerization [3]. The proteolytic processing of Gag follows a sequential cascade of events that is kinetically controlled by differential rates of processing at each of the five cleavage sites in Gag [4,5]. Protease-mediated Gag–Pol processing requires the protease as well as domains upstream or downstream of the protease region, such as the reverse transcriptase (RT) and integrase (IN) domains. Mutants with an IN-domain deletion form markedly impaired viral particles due to the impairment of normal protease activity [6]. Mature HIV-1 RT is a heterodimer with two subunits, p66 and p51. The p51 subunit is derived from p66 by the proteolytic removal of the C-terminal RNaseH domain. RT–RT interactions may play important roles in protease activation by promoting Gag–Pol multimerization. RT inhibitors enhance RT dimerization in vitro, resulting in increased protease-specific cleavage of Pr55-Gag and Gag–Pol [7]. However, the deletion of the RT region leads to a marked reduction in protease activation and particle maturation [8]. The critical amino acid residues of the HIV-1 RT that contribute to protease-mediated Gag–Pol processing are not yet known.

In this study, we identified the HIV-1 RT amino acid residues critical for Gag–Pol processing through the analysis of RT phosphorylation. The substitution of Thr-128 and Tyr-146 with Ala severely impaired viral replication, due to defects in proteolytic processing at the MA/CA, p66/p51, and RT/IN sites.

2. Materials and methods

2.1. Plasmids

Details of the plasmid constructs used in this study are provided in the Supplementary materials and methods.

2.2. Virus infection

For infection, 293T cells were co-transfected with 0.1 μg of pMD.G-VSV-G and 0.1 μg of pNL43lucΔenv or pNL43lucΔenv

Abbreviations: HIV-1, human immunodeficiency virus type 1; RT, reverse transcriptase; DTSSP, 3,3′-dithiobis(sulfosuccinimidylpropionate); PR, protease

* Corresponding authors. Address: Department of Life and Environmental Sciences, Chiba Institute of Technology, 2-17-1 Tsudanuma, Narashino, Chiba 275-0016, Japan (H. Takaku). Fax: +81 47 478 0407.

E-mail addresses: hironori.nishitsuji@it-chiba.ac.jp (H. Nishitsuji), hiroshi.takaku@it-chiba.ac.jp (H. Takaku).

0014-5793/$36.00 © 2011 Federation of European Biochemical Societies. Published by Elsevier B.V. All rights reserved.
doi:10.1016/j.febslet.2011.09.034

containing an RT mutation of interest. At 48 h post-transfection, the culture supernatants were harvested and filtered through 0.45-μm filters. 293T cells were infected with pseudotyped viruses (corresponding to 20 ng of p24). At 24 h postinfection, the cells were harvested and lysed with 300 μl of cell-lysis buffer. An aliquot (10 μl) of each lysate was then subjected to a luciferase assay.

2.3. Preparation of virions

Details are given in the Supplementary materials and methods.

2.4. Preparation of anti-RT sera

Details of anti-RT sera used in this study are given in the Supplementary materials and methods.

2.5. Crosslinking

Crosslinking was performed as previously described [9].

2.6. Phosphorylation assay

Details are given in the Supplementary materials and methods.

3. Results

3.1. Infectivity of RT-mutant viruses

Recent studies have indicated that the phosphorylation of HIV-1 RT might play an important role in HIV-1 replication [10–11]. To evaluate the role of the putatively phosphorylated RT, we predicted the phosphorylation site(s) of RT using the Scansite 2.0 program [12] and generated single-amino-acid Ala substitutions for the Ser, Thr, and Tyr residues that are conserved among HIV-1 and simian immunodeficiency virus strains. We examined the effect of each mutation on viral replication using a single-round infection system (Fig. 1A). In this study, infection with the S156A mutant led to slightly diminished luciferase activity (approximately 75% of the WT level). Similarly, the single amino acid substitutions of Thr to Ala at position 27 (T27A) and Ser to Ala at position 68 or 105 (S68A and S105A, respectively) resulted in lower levels of luciferase activity (60–65% of the WT level). The infectivity of the RT mutant virus possessing a T58A or T107A mutation significantly decreased to 5–10% of the WT-virus level. The introduction of the T131A, T216A, Y318A, T128A, Y146A or Y183A mutations completely abolished viral infectivity.

To evaluate whether HIV-1 RT mutations affect RT activity, we used the Vpr-p66-WT fusion protein (Fig. 1B), which can be efficiently incorporated into virions [13–14]. The infectivity of T58A, T216A and Y318A was partially restored from 27% to 55% of the WT infectivity by complementation with Vpr-p66-WT-V5 (Fig. 1C). In this complementation, Vpr-p66-WT-V5 was efficiently packaged and processed (Fig. 1E). The T107A mutant was not complemented by Vpr-p66-WT-V5. In addition, the level of RNaseH-V5 in T107A was significantly decreased compared with the WT virion, although the Vpr-p66-WT-V5 and p66-WT-V5 levels in the T107A mutant were similar to WT levels. Moreover, the T131A, and Y183A mutations, which resulted in lower levels of p66-WT-V5 and RNaseH-V5, were not complemented despite the presence of Vpr-p66-WT-V5 (1.3–3.5% of the WT level). In the T128A and Y146A mutants, the majority of Vpr-p66-WT-V5 in the virions remained in the form of unprocessed fusion proteins, and these mutants exhibited defective viral replication (0.5–3.1% of the WT level). To further examine whether incorporating Gag–Pol-WT *in trans* restores the infectivity of the mutant viruses, Gag–Pol-complemented viruses were analyzed for infectivity using a luciferase assay (Fig. 1D). With the exception of Y183A, mutant virus infectivity was partially rescued (26–75% of WT level) by this complementation. Of particular note, a Y183A mutation incorporated into the WT Gag–Pol did not complement infectivity. This result was due to the p66-Y183A mutation displaying some inhibitory potency, as indicated by Vpr-p66-Y183A packaging into the WT virion (data not shown). We concluded that the replication defects associated with the T58A, T216A and Y318A mutants were due primarily to the disruption of RT activity, whereas Thr-107, Thr-128, Thr-131, Tyr-146, and Tyr-183 may be involved in Gag–Pol functions in HIV-1 replication.

3.2. Mutations of Thr-128 and Tyr-146 in RT abolish Gag–Pol processing

To study whether the mutant RTs in the viral particles were present in the p66 and p51 form of the RT, we used anti-RT serum to detect virus-associated mutant RTs (Fig. 2A). The T128A, T131A and Y146A mutations were not found in the p51 form of the RT. Although all of the mutant RTs in the viral particles were detected in the p66 form, T128A, T131A, Y146A, and Y318A mutants had slightly reduced levels of the p66 form relative to the WT. These mutants may be subject to PR-mediated degradation [15].

We next examined the profiles of particle-associated viral proteins to identify possible Gag–Pol processing defects in these mutants. The majority of the Gag-related proteins in the T128A and Y146A mutant virions remained as unprocessed Pr55-Gag (Fig. 2B). The defective Gag-processing phenotype of the T128A and Y146A virions was apparent from the altered ratio of the Pr55-Gag and p24 forms of the CA protein (Fig. 2C). Moreover, the protein levels of HIV-1 protease and integrase were significantly reduced in the T128A and Y148A virions (Fig. 2D and E). Thus, a single amino-acid substitution for Thr-128 or Tyr-148 in the RT appeared to be responsible for the observed effects on Gag–Pol processing.

3.3. Proteolytic cleavage of Gag–Pol was severely impaired at the MA/CA and RT/IN sites in T128A and Y146A virions

To determine the defective sites of Gag–Pol processing in detail, we incorporated several truncated Gag or Pol domains into HIV-1 virions *in trans* as fusion partners of Vpr (Fig. S1A). The proportion of the processed products cleaved at the MA/CA and RT/IN sites was significantly reduced in T128A and Y146A mutants (Fig. S1B and F). In contrast, the cleavage patterns for the SP1/NC, NC/SP2, and SP2/P6 sites in T128A and Y146A mutants were similar to those of the WT (Fig. S1C, D and E). These results suggest that protease-mediated Gag–Pol processing in T128A and Y146A virions was partially affected, but these mutants retained protease activity.

3.4. HIV-1 Gag–Pol processing is dependent on RT dimerization

To determine whether RT dimerization was required for Gag–Pol processing, we used DTSSP (3,3′-dithiobis(sulfosuccinimidylpropionate)) to cross-link protein complexes present in the RT-V5-expressing 293T cells. Only RT monomers were detected in the non-cross-linked samples, with the exception of the Y146A mutant. The addition of 0.2 mM DTSSP yielded cross-linked complexes of RT homodimers when RT-WT-V5 was expressed in 293T cells (Fig. 3). A T131A mutation slightly reduced the level of RT homodimers in the presence of DTSSP compared with the wild type. In contrast, an abnormal pattern was observed in the Y146A mutant in the absence or presence of DTSSP, suggesting that Y146A induced improper folding. Moreover, a T128A mutation resulted in very low levels of the dimer under the same experimental conditions. T58A, Y183A and T216A mutations, which resulted in normal Gag–Pol, retained RT dimerization in the presence of DTSSP. These results suggest that

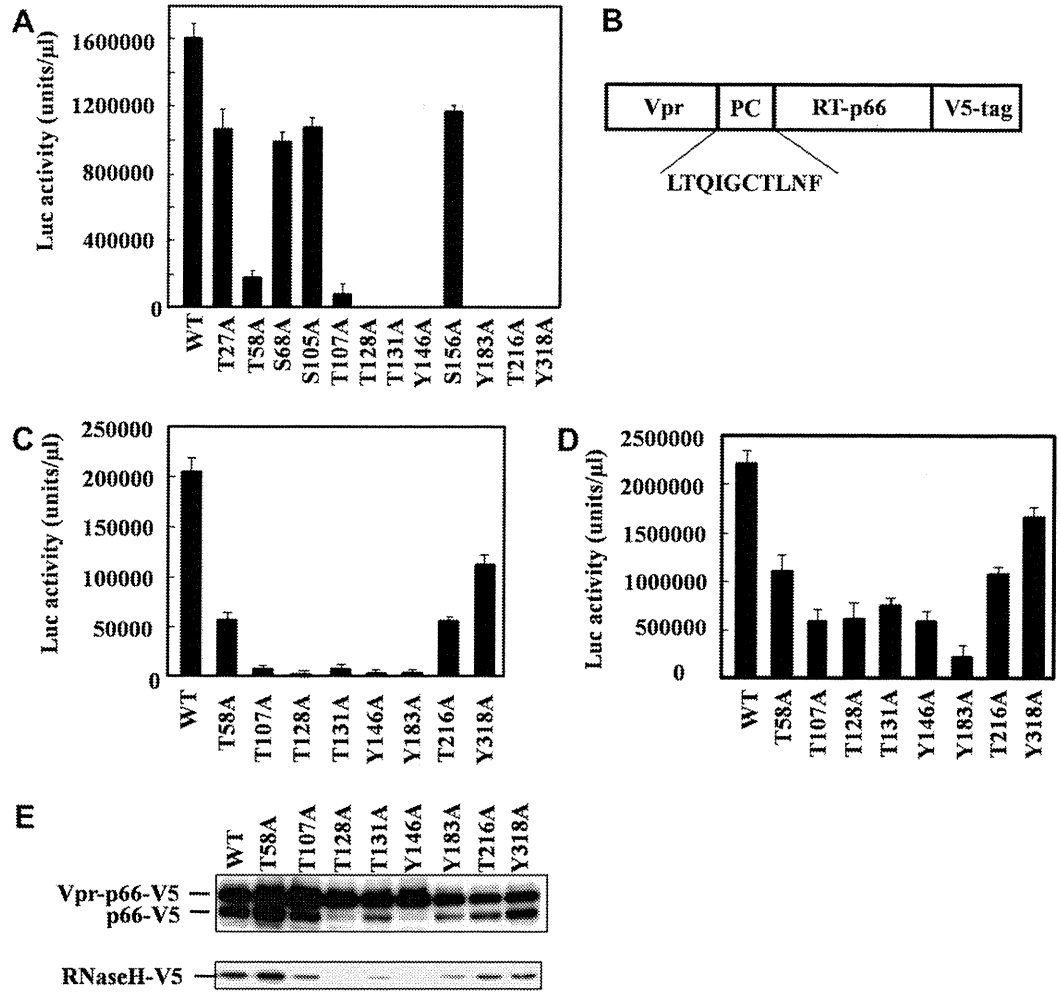

Fig. 1. Infectivity of HIV-1 RT mutants. (A) 293T cells were transfected with 0.1 μg of pMD.G-VSV-G and 0.1 μg of pNL43lucΔenv containing the indicated RT mutations. The 293T cells were infected by pseudoviruses isolated from cell culture supernatants. The luciferase activity in the infected cells was measured 24 h postinfection. (B) An illustration of the Vpr-p66-WT fusion protein including ten amino acids of the protease cleavage sequence at the Vpr-RT junction. (C, D) The 293T cells were transfected with 0.1 μg of wild type (WT) or each RT mutant pNL43lucΔenv, 0.1 μg of pMD.G-VSV-G and 0.2 μg of pVpr-p66-WT-V5 (C) or pMDL-g/p-RRE (D). At 48 h post-transfection, the 293T cells were infected with the indicated pseudotyped viruses. Luciferase activities in the infected cells were measured 24 h postinfection. (E) Culture supernatants in Fig. 1C were collected and subjected to Western immunoblot analysis using an anti-V5 antibody.

RT dimerization may affect Gag–Pol processing. However, the possibility that the T128A and Y146A mutations significantly change the conformation of Gag–Pol precursor, decreasing the accessibility of the targets, cannot be excluded.

3.5. Detection of RT phoshorylation

Harada et al. have reported that HIV RT can be phosphorylated in vitro by casein kinase 2 (CK2-alpha) [16]. We used Phos-tag SDS–PAGE to determine whether CK2-alpha could phosphorylate HIV-1 RT. A phos-tag binds to two Mn^{2+} ions and acts as a phosphate-binding molecule [17]. This complex is used for phosphate affinity SDS–PAGE, in which a mobility shift can be observed with phosphorylated proteins. Recombinant His-RT was incubated with recombinant CK2-alpha in the presence of ATP. As shown in Fig. 4A, a shifted band of recombinant His-RT-WT was observed in the presence of recombinant CK2-alpha in a dose-dependent manner. We next examined the phosphorylation of mutant RT. The phosphorylation levels of His-RT-T128A were similar to wild-type RT (Fig. 4B). In the case of the His-RT-Y146A mutants, the phosphorylation levels were slightly reduced compared with wild-type levels. Moreover, both the T128A and Y146A mutations in recombinant His-RT severely decreased the phosphorylation levels. However, a shifted band corresponding to phosphorylated His-RT-T128A-Y146A could be detected by using a large amount of recombinant His-RT-T128A-Y146A in an in vitro kinase assay (Fig. 4C). To further confirm the phosphorylation of HA-RT-wild and its RT mutants in vivo, HA-tagged RT or its mutants were expressed in 293T cells and the cell lysates were immunoprecipitated with anti-HA antibody. The immune complex was analyzed by Phos-tag, a probe used to detect phosphorylated proteins (Fig. 4D). Wild-type RT was phosphorylated in vivo. However, RT-T128A-Y146A significantly reduced the phosphorylation levels. These results suggest that the T128 and Y146 residues, but not the RT phosphorylation sites, which demonstrated a defect in RT dimerization, affected RT phosphorylation. RT phosphorylation may be required for its dimerization.

4. Discussion

Dunn et al. have reported that an L264S or E302Q mutation in RT rendered the protein susceptible to degradation by PR within virions [15]. In contrast, we identified here the critical amino acid residues (T128 and Y146) that specifically affected RT dimerization but had little effect on the stability of RT. To obtain structural insights into the findings, we constructed a 3-D model of p51/p66 heterodimer of the wild-type (NL43) RT. The model shows that

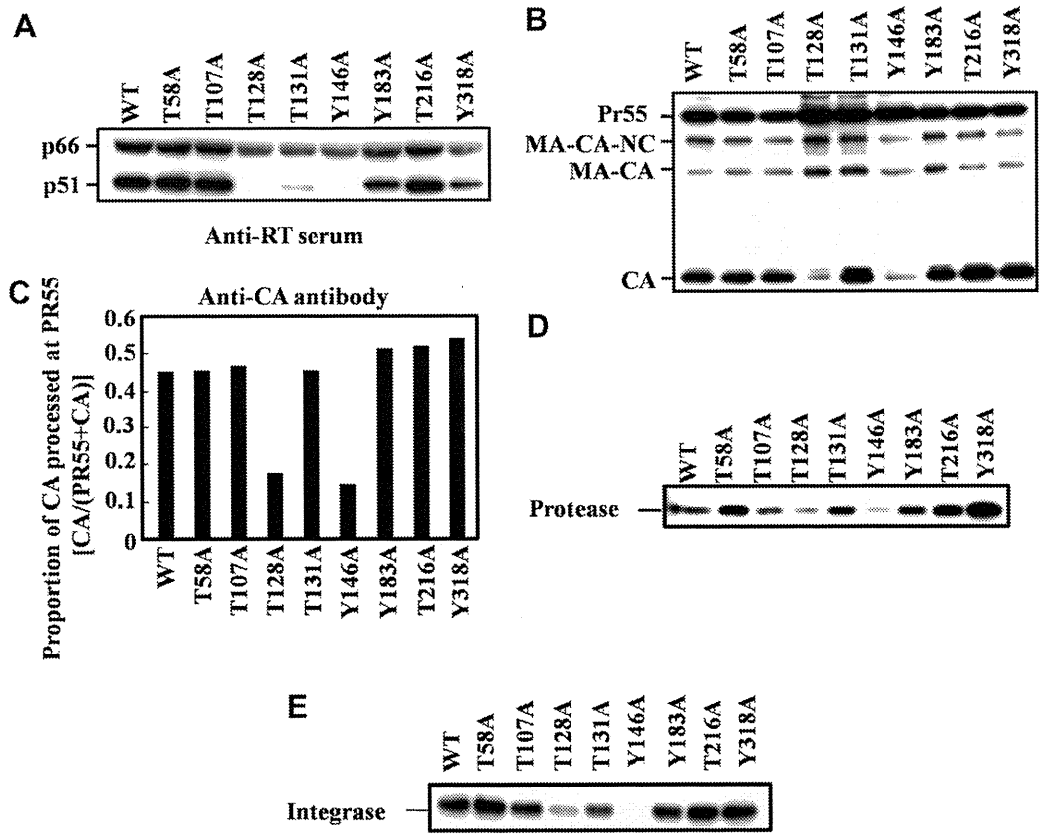

Fig. 2. The effect of RT mutations on the processing of HIV-1 Gag–Pol. 293T cells were transfected with 0.2 μg of each RT mutant pNL4-3. At 48 h post-transfection, the supernatants were harvested and subjected to Western-blot analysis. The Gag–Pol cleavage products were detected using anti-RT sera (A), an anti-CA antibody (B), an anti-protease antibody (D) and an anti-integrase antibody (E). (C) The proportion of CA cleaved at the Pr55-Gag cleavage site was calculated from the integrated band intensities.

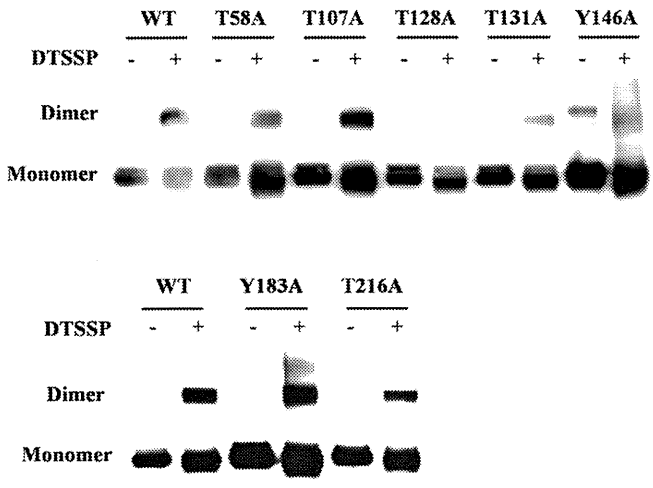

Fig. 3. Evaluation of RT dimerization. 293T cells were transfected with pLenti-p66-V5 or the RT mutants. At 48 h post-transfection, the cells were lysed with CSK buffer containing 0.5% NP-40. The cell lysates were incubated in either the absence or presence of 0.2 mM DTSSP at room temperature for 20 min and analyzed by Western blotting using an anti-V5 antibody.

the L264 and E302 residues are located in the two α-helixes of Thumb domain (Fig. S2A). Because helices are often critical in formation of a stable core structure of a protein, the L264S or E302Q mutations could critically influence proper folding and stability of the Thumb domain. Such effects could affect RT dimerization because the thumb of the p51 subunit extensively interacts with the RNase H domain. Simultaneously, the effects could increase susceptibility of mutants to PR in a virion via exposure of improperly folded domain. In contrast, the T128 and Y146 residues in p51 are positioned at the base of the β7–β8 loop, whose tip is embedded in a small cleft of p66 surface and constituted of a direct interaction surface between p51 and p66 (Fig. S2B). Therefore mutations at T128 and Y146 could influence orientation of the β7–β8 loop and alter stability of the RT dimer. Meanwhile, the mutations would not influence critically the stability of the RT, because the loop is positioned on protein surface. The failure of detection of RT p51 subunit in these mutants (Fig. 2A) may suggest that p66 dimerization is prerequisite for the processing. These structural insights are well consistent with the present experimental findings. However, further studies will be required to clarify the structure–function relationship with regard to the susceptibility of RT to PR degradation.

The mutation of T128 or Y146 in RT impaired the protease-mediated Gag–Pol processing. It is possible that substitutions in RT significantly change the conformation of the Gag–Pol precursor and decrease the accessibility of the targets for the protease. However, the three-dimensional (3-D) model suggests that the T128 and Y146 residues are not positioned near the inherent cleavage sites flanking RT, i.e., N- and C-terminal end of the RT (Fig. S2). In addition, reported electron microscopy studies suggest that Gag precursor has a rodlike structure [18,19], by which the T128 and Y146 residues are probably located far from the cleavage site and other proteins. Therefore, the mutations at the T128 and Y146 are less likely to influence critically the protease accessibility into the inherent cleavage sites of the Gag/Pol precursor protein, although the influences are formally not ruled out at present. An

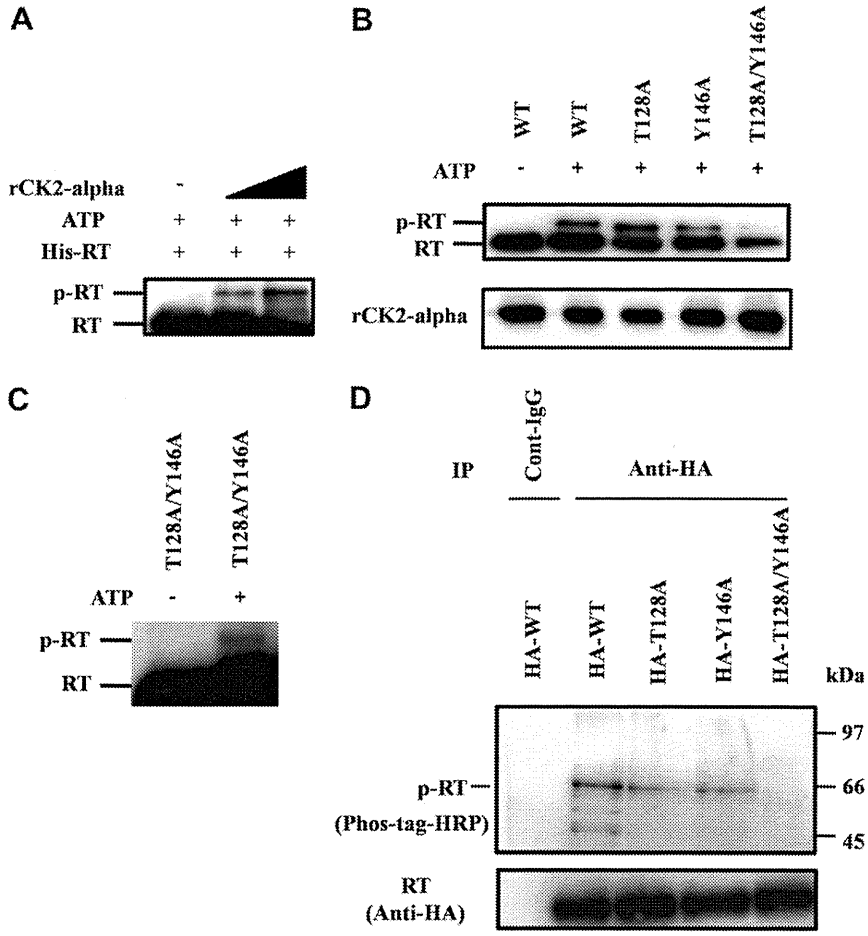

Fig. 4. The phosphorylation of recombinant RT in vitro. (A) Initially, 0.1 μg of recombinant His-RT-WT was incubated with 0.5 mM ATP in the absence or presence of 0.05 or 0.2 μg of recombinant His-CK2-alpha. The phosphorylation of recombinant His-RT was detected using Western immunoblot analysis after Phos-tag SDS–PAGE. The phosphorylation of the recombinant His-RT was indicated as a shifted band. (B, C) 0.1 μg (B) or 1.0 μg (C) of indicated recombinant His-RT was incubated with 0.2 μg of recombinant His-CK2-alpha in the absence or presence of 0.5 mM ATP. The phosphorylation of His-RT was detected as indicated in Fig. 4A. (D) 293T cells were transfected with pcDNA-HA-RT or its RT mutants. At 48 h after transfection, the cells lysates were immunoprecipitated with anti-HA antibody and phosphorylated proteins were detected using Phos-tag-Biotin and Streptavidin-conjugated HRP.

alternative possibility is that the mutations at the T128 and Y146 impaired the protease-mediated Gag–Pol processing via attenuation of Gag/Pol dimerization for PR activation. Further study is necessary to address each of these issues.

These observations are consistent with the hypothesis that antiviral drugs targeting RT might inhibit HIV-1 replication without necessarily inhibiting the catalytic function of the RNA-dependent DNA polymerase.

Acknowledgments

We thank Dr. I.S.Y. Chen for providing pNL4-3lucΔenv and Dr. H. Miyoshi for providing pMD.G-VSV-G. This work was supported by a Grant-in-Aid for AIDS research from the Ministry of Health, Labor, and Welfare, Japan, a Grant-in-Aid for High Technology Research (HTR) from the Ministry of Education, Science, Sports, and Culture, Japan, and a Grant from the Strategic Research Foundation Grant-aided Project for Private Universities from the Ministry of Education, Culture, Sport, Science, and Technology, Japan (MEXT).

Appendix A. Supplementary data

Supplementary data associated with this article can be found, in the online version, at doi:10.1016/j.febslet.2011.09.034.

References

[1] Jacks, T., Power, M.D., Masiarz, F.R., Luciw, P.A., Barr, P.J. and Varmus, H.E. (1988) Characterization of ribosomal frameshifting in HIV-1 gag-pol expression. Nature 331, 280–283.
[2] Park, J. and Morrow, C.D. (1992) The nonmyristylated Pr160gag-pol polyprotein of human immunodeficiency virus type 1 interacts with Pr55gag and is incorporated into viruslike particles. J. Virol. 66, 6304–6313.
[3] Louis, J.M., Nashed, N.T., Parris, K.D., Kimmel, A.R. and Jerina, D.M. (1994) Kinetics and mechanism of autoprocessing of human immunodeficiency virus type 1 protease from an analog of the Gag-Pol polyprotein. Proc. Natl. Acad. Sci. USA 91, 7970–7974.
[4] Wiegers, K., Rutter, G., Kottler, H., Tessmer, U., Hohenberg, H. and Krausslich, H.G. (1998) Sequential steps in human immunodeficiency virus particle maturation revealed by alterations of individual Gag polyprotein cleavage sites. J. Virol. 72, 2846–2854.
[5] Pettit, S.C., Everitt, L.E., Choudhury, S., Dunn, B.M. and Kaplan, A.H. (2004) Initial cleavage of the human immunodeficiency virus type 1 GagPol precursor by its activated protease occurs by an intramolecular mechanism. J. Virol. 78, 8477–8485.
[6] Bukovsky, A. and Gottlinger, H. (1996) Lack of integrase can markedly affect human immunodeficiency virus type 1 particle production in the presence of an active viral protease. J. Virol. 70, 6820–6825.
[7] Tachedjian, G., Moore, K.L., Goff, S.P. and Sluis-Cremer, N. (2005) Efavirenz enhances the proteolytic processing of an HIV-1 pol polyprotein precursor and reverse transcriptase homodimer formation. FEBS Lett. 579, 379–384.
[8] Quillent, C., Borman, A.M., Paulous, S., Dauguet, C. and Clavel, F. (1996) Extensive regions of pol are required for efficient human immunodeficiency virus polyprotein processing and particle maturation. Virology 219, 29–36.
[9] Nishitsuji, H., Hayashi, T., Takahashi, T., Miyano, M., Kannagi, M. and Masuda, T. (2009) Augmentation of reverse transcription by integrase through an